https://doi.org/10.5194/egusphere-2023-778
Preprint. Discussion started: 25 April 2023

High-frequency variability dominates potential connectivity between remote coral reefs

Noam S. Vogt-Vincent[1], Satoshi Mitarai[2], and Helen L. Johnson[1]

[1]Department of Earth Sciences, South Parks Road, University of Oxford, Oxford, UK
[2]Marine Biophysics Unit, Okinawa Institute of Science and Technology Graduate University, Tancha, Okinawa, Japan

Correspondence: Helen Johnson (helen.johnson@earth.ox.ac.uk)

Abstract. Coral larval dispersal establishes connectivity between reefs, but larval fluxes vary over timescales from daily to multidecadal due to oceanographic variability. Using a 2km-resolution ocean model, we simulate daily spawning events from 1993-2019 (for a total of almost 10,000 events) across all coral reefs in the tropical southwest Indian Ocean. Although there is a significant seasonal cycle in potential connectivity at many reefs, day-to-day variability generally dominates. The importance of this day-to-day variability depends on the local geography and oceanography. Stochastic oceanographic variability introduces considerable uncertainty to dispersal predictions, imposing significant limitations on what dispersal simulations can tell us about connectivity. Protracted spawning over only a few days can significantly reduce variability associated with the likelihood of a larva settling successfully. The duration of spawning is therefore likely a more important parameter in modelling coral connectivity than the exact timing of spawning onset. Finally, we find that a small proportion of spawning events account for the majority of successfully settling larvae, particularly at remote islands, and demonstrate that a time-mean picture of dispersal may be inappropriate for predicting demographic and genetic connectivity.

1 Introduction

Although mature corals are sessile, connectivity can be established between coral reefs through the drift of coral larvae, which are generated in enormous numbers by broadcast-spawning corals (e.g. Harrison, 2010). Larval dispersal is a key process in coral reef ecology. If the physical transport of larvae between reefs (potential connectivity) affects population growth rates, reefs become demographically connected (Lowe and Allendorf, 2010). For instance, reefs that act as larval sinks may have an improved capacity to recover from environmental disturbances, and key larval sources are therefore important for reef system resilience (Hock et al., 2017; Gouezo et al., 2019). These metrics are increasingly incorporated into conservation planning and the design of marine protected areas (Balbar and Metaxas, 2019; Harrison et al., 2020; Goetze et al., 2021). Dispersal is also important for long-term resilience to environmental change if it results in genetic connectivity, due to the exchange of genotypes adapted to different environmental conditions (Kleypas et al., 2016; McManus et al., 2021).

Despite its importance, coral larval dispersal is challenging to quantify (Edmunds et al., 2018). Directly tracking coral larval transport is currently only possible at local scales (Doropoulos and Roff, 2022; Geertsma et al., 2023). Genetic indices can be used to infer migration rates between populations, but these approaches can struggle with low genetic differentiation

https://doi.org/10.5194/egusphere-2023-778
Preprint. Discussion started: 25 April 2023

characteristic of many marine organisms, are generally resource intensive, and have limited capacity to capture connectivity variability (Faubet et al., 2007; Lowe and Allendorf, 2010; Samarasin et al., 2017). For corals, numerically modelling larval dispersal, usually through Lagrangian approaches, is therefore the primary source of dispersal estimates for coral connectivity. Numerous such studies have been carried out over the past couple of decades (e.g Galindo et al., 2006; Wood et al., 2014; Thompson et al., 2018).

Coral larval dispersal is a coupled biological and physical process. Transport is largely driven by physical ocean currents as coral larvae are, to first-order, weak swimmers (Kingsford et al., 2002; Hata et al., 2017). Coral larvae have a limited competency window (usually on the order of days to weeks), outside of which they are unable to settle, and also die following a time-dependent mortality rate (Graham et al., 2008; Connolly and Baird, 2010). Early work often modelled larval dispersal as a time-independent advection-diffusion process, multiplied by functions incorporating competency and survival dynamics (Largier, 2003; Connolly and Baird, 2010). However, this static picture of potential connectivity contradicts observations of coral recruitment rates that can vary by orders of magnitude between years (e.g. Porter and Schleyer, 2017; Thomson et al., 2021; Adjeroud et al., 2022). In fact, the time-varying flow field in the ocean introduces a significant stochastic component to potential connectivity (Siegel et al., 2008; Mitarai et al., 2008), where connectivity occurs in pulses driven by the filamentation of larvae in regions of high strain and current convergence (Harrison et al., 2013; Dauhajre et al., 2019).

As broadcasting scleractinian corals generally spawn infrequently in short-duration spawning events (Baird et al., 2009), most numerical modelling studies simulate spawning during a certain known (or suspected) spawning period, repeated annually over a certain number of years. Potential connectivity is then often integrated across each spawning period, with some studies focusing on the time-mean or seasonal picture (e.g. Wood et al., 2014; Gamoyo et al., 2019), whilst others also investigate interannual variability, with varying degrees of complexity (e.g. Treml et al., 2008; Wood et al., 2016; Thompson et al., 2018). It is clear from the considerable effort that has gone into modelling coral larval dispersal that potential connectivity varies over a wide range of timescales, but few studies have investigated the consequences of high-frequency potential connectivity variability for ecological applications.

Consider the fate of a larval packet generated by a particular coral species at a particular reef site. Perhaps we are fortunate, and precisely know that spawning starts on day t every year (maybe we even know the exact time), taking place over Δt days. This may appear to be a very useful initial condition. However, in the absence of extremely good data assimilation at an appropriate scale, or dominant oceanographic processes that are inherently predictable (e.g. a tidal lagoon), there is a strong stochastic component to short-term larval transport (Siegel et al., 2008; Mitarai et al., 2008). Even with appropriate data assimilation, the chaotic nature of turbulent flow results in uncertainty associated with larval position growing rapidly with time (e.g. Romero et al., 2013). A biophysical larval dispersal model hopefully captures the statistical properties of the turbulent flow, but the state of the system is highly unlikely to be correct at any one time. As a result, even in this best case scenario, quantifying the magnitude and timescales of this stochastic variability is essential for understanding uncertainty in potential connectivity predictions.

In many cases, however, the spawning timing and duration may *not* be precisely known. In the southwest Indian Ocean, temporal and spatial coverage of spawning observations is very poor (Baird et al., 2021). It is therefore also important to

https://doi.org/10.5194/egusphere-2023-778
Preprint. Discussion started: 25 April 2023

understand the magnitude and effects of seasonality on reef potential connectivity. This could be particularly influential for the Indian Ocean, where monsoonal winds lead to a seasonal reorganisation of surface currents (Schott and McCreary, 2001), and therefore potential connectivity, between the northwest monsoon in the austral summer and southeast monsoon in the austral winter.

In addition to seasonality, connectivity may also vary from year to year. For instance, Thompson et al. (2018) demonstrated that at least 20 years of data were required to capture the interannual potential connectivity variability in the Coral Triangle (maritime southeast Asia) region. However, given that Thompson et al. (2018) only considered two short spawning events per year, it is not clear to what extent this interannual variability in connectivity reflects long-frequency oceanographic variability, as opposed to being a sampling artefact due to the aliasing of high-frequency variability.

Regardless of its origin, stochastic variability in potential connectivity strongly affects metapopulation dynamics (Watson et al., 2012), but beyond the expectation of a seasonal cycle (Gamoyo et al., 2019), little is known about the magnitude, timescales, geography, or physical drivers of this variability in the southwest Indian Ocean. As a result, in this study, we set out to answer the following key questions:

1. How does potential connectivity vary over day-to-day, seasonal, and interannual timescales across the southwest Indian Ocean?
2. What are the physical oceanographic drivers of this variability?
3. To what extent is this variability important for understanding demographic and genetic connectivity?

To answer these questions, we present a modelled potential connectivity time-series, spanning all coral reefs in the tropical southwest Indian Ocean, as a function of spawning time. We consider larval fluxes between over eight thousand 4km^2 reef cells, across 27 years (for a total of almost 10,000 individual daily spawning events), based on a state-of-the-art 2km-resolution regional ocean model (Vogt-Vincent and Johnson, 2023). This is the highest resolution (spatial and temporal) connectivity dataset ever generated in this region, allowing us to carry out a detailed investigation into the temporal variability of reef potential connectivity across scales and oceanographic regimes. The potential connectivity matrices and hydrodynamic data used in this study are freely available, and our analyses can be rerun under different biological parameterisations using the associated code (see *code and data availability*).

2 Methods

2.1 Hydrodynamical and larval dispersal models

We generated potential connectivity matrices for coral larval dispersal across the southwest Indian Ocean using SECoW (Simulating Ecosystem Connectivity with WINDS). SECoW is a modelling system combining hydrodynamic data from WINDS-M (Vogt-Vincent and Johnson, 2023), a regional ocean simulation for the southwest Indian Ocean, with a larval dispersal model

https://doi.org/10.5194/egusphere-2023-778
Preprint. Discussion started: 25 April 2023

based on OceanParcels (Lange and van Sebille, 2017; Delandmeter and van Sebille, 2019). WINDS-M is a 1/50° configuration of the CROCO ocean model (Auclair et al., 2019) spanning all coral reefs in the southwest tropical Indian Ocean, and is described and validated in Vogt-Vincent and Johnson (2023). WINDS-M is forced at the boundaries by the CMEMS 1/12° global ocean reanalysis and analysis (Lellouche et al., 2021) and 10 tidal constituents (elevations and barotropic currents) from the TPXO9-atlas (Egbert and Erofeeva, 2002), and at the surface by the ERA-5 atmospheric reanalysis (Hersbach et al., 2020). SECoW uses 30-minute frequency surface current output from WINDS-M for the years 1993-2020, thereby resolving hydrodynamic variability ranging from tidal to interannual.

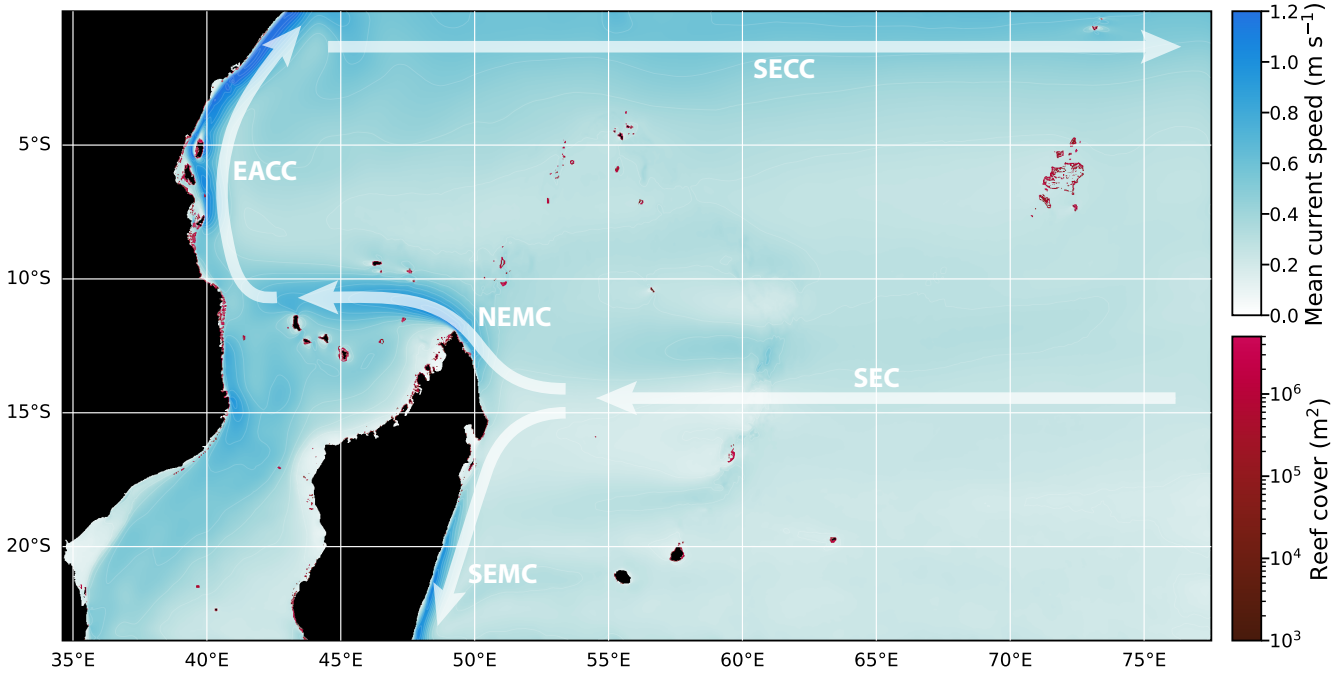

Figure 1. The model domain investigated in this study, with the time-mean surface current speed (blues) and reef surface area per grid cell (reds). Also shown is a schematic representation (after Schott et al. (2009)) of the major ocean currents in the region, namely the South Equatorial Current (SEC), Northeast Madagascar Current (NEMC), Southeast Madagascar Current (SEMC), East Africa Coastal Current (EACC), and South Equatorial Countercurrent (SECC). Note that circulation in the Mozambique Channel is dominated by eddies, wind-driven surface currents often reverse at the equator and, during the northwest monsoon, the southward-flowing Somali Current enters the domain and meets the East Africa Coastal Current between 0-5° S.

The larval dispersal component of SECoW assumes that coral larvae physically behave as positively buoyant, otherwise passive particles, which are advected by surface currents for 120 days after spawning, using a fourth-order explicit Runge-Kutta scheme in OceanParcels. We identifed 8088 2×2 km reef cells on the WINDS grid (Figure 1), and released 1024 particles per cell per day, simulating daily spawning events at midnight from 1 January 1993 to 31 December 2019, for a total of 9861 domain-wide spawning events. Particles represent a number of larvae proportional to the reef area of their source cell

https://doi.org/10.5194/egusphere-2023-778
Preprint. Discussion started: 25 April 2023

(i.e. assuming constant fecundity per unit area of reef). Following Connolly and Baird (2010), we assumed that coral larvae gain and lose competency at constant rates after a minimum competency period, and die following a time-dependent mortality rate. We further assumed that competent larvae settle at a rate proportional to the reef cover in the occupied cell. This accounts for the capacity of upstream reefs to reduce the larval supply to downstream reefs, whilst sensibly handling sub-grid scale reef coverage and allowing for the possibility of a larva passing over a reef without settling (Hata et al., 2017). Biological parameters are based on *Platygyra daedalea* (Supplementary Figure 1, Supplementary Table 1). The results described in this study are robust with respect to biological paramaters (Supplementary Table 2), but alternate versions of the figures in this manuscript for the other four coral species described in Connolly and Baird (2010) are included in the Supplementary Dataset 1.

In this study, we computed two key metrics:

- **Flux**, $\boldsymbol{F}_{ijk}$: The number of larvae spawning from location i at event k, and settling at location j.
- **Source strength**, $\boldsymbol{S}_{ik}$: The proportion of larvae from location i and spawning event k that settle anywhere.

Aside from the particle behaviour (passive), all biological parameters (including reef fecundity, settling rate, mortality parameterisations, etc) can be changed using the associated scripts and data (Supplementary Datasets 1 and 2), without the need to rerun expensive Lagrangian simulations.

In Section 3, we focus on the source strength matrix $\boldsymbol{S}_{ik}$ for individual reef cells. Contrary to flux, source strength is a function of just one location (rather than a pair of locations), so it is more straightforward to investigate geographic dependence. In Section 4, we also consider the flux matrix $\boldsymbol{F}_{ijk}$ for reef groups. The full flux matrix in SECoW has $8088 \times 8088 \times 9861 \approx 645 \times 10^9$ elements so, for tractability, we have formed 180 reef groups (see Supplementary Dataset 1) using an agglomerative clustering algorithm, resulting in a more manageable $180 \times 180 \times 9861$ matrix. Full details can be found in Supplementary Texts 1-3.

2.2 Data analysis

2.2.1 High-frequency variability

We quantified the high-frequency (day-to-day) variability of source strength as the 1 day lagged temporal autocorrelation, $r_{1\mathrm{d}}$. If $r_{1\mathrm{d}}$ is high, source strength on day k is a good predictor of the source strength on day $k+1$. Conversely, low $r_{1\mathrm{d}}$ indicates very high day-to-day reef connectivity variability. Examples are shown in Figure 2(c-e); for instance, compare the relatively steady source strength near Tanga in Tanzania ($r_{1\mathrm{d}} = 0.86$) to the sporadic source strength at Rémire Island in Seychelles ($r_{1\mathrm{d}} = 0.24$). We computed $r_{1\mathrm{d}}$ independently for each cell, using the full 1993-2019 daily time-series.

To investigate the physical drivers of $r_{1\mathrm{d}}$, we first split all reef cells into six groups based on their hydrogeography, as different physical drivers may dominate in different oceanographic regimes. These groups are (1) reefs influenced by the EACC; (2) Mozambique; (3) Madagascar; (4) remote islands and reefs near the NEMC; (5) other remote islands; and (6) the Chagos Archipelago (Figure 1). Within each group, we then carried out ordinary least-squares (OLS) regression with 7 potential

https://doi.org/10.5194/egusphere-2023-778
Preprint. Discussion started: 25 April 2023

explanatory variables we hypothesised could explain spatial variation in r_{1d}, using the `statsmodels` Python package. These explanatory variables were (1) mean surface current speed, (2) mean surface high-frequency (1/30 – 1 d^{-1}) current speed, (3) mean surface sub-daily current speed, (4) nearby reef fraction, (5) weighted downstream connection distance, (6) distance to land, and (7) mean source strength. Technical details can be found in Supplementary Text 4. These variables were all strongly positively skewed, so we used the logarithm in the regression calculation. We identified the strongest explanatory variable on the basis of the R^2 value. Finally, to test whether the 'best' identified explanatory variable is substantially stronger than the others, we carried out multivariate OLS regressions using every pair of explanatory variables. We did not use OLS models with more than two explanatory variables, as we did not think that more complex models would provide significantly more physical insight.

2.2.2 Seasonal variability

To assess the strength of the regular seasonal cycle in source strength, we computed the correlation for each reef cell between monthly mean source strength and the regular seasonal cycle (i.e. the monthly climatological source strength) averaged across 1993-2019, specifically extracting the R^2 value. We also carried out an Empirical Orthogonal Function (EOF) analysis of the monthly-mean source strength matrix, decomposing the time-varying matrix into a set of principal components and associated basis functions. A similar analysis was previously carried out by Thompson et al. (2018) to investigate interannual connectivity variability. In our analyses, the first principal component (PC1) always corresponded to a seasonal cycle. To investigate how connectivity variability across the southwest Indian Ocean responds to the seasonal cycle, we then computed the correlation of the monthly-mean source strength time-series at each reef cell with PC1, $r_{\mathrm{PC1},S}$. To interpret the physical oceanographic drivers of this variability, we also computed the correlation between PC1 and the monthly-mean surface current speed, and the zonal u and meridional v components of the surface current velocity. The latter results in a new vector field, $(r_{\mathrm{PC1},u}, r_{\mathrm{PC1},v})$, returning the correlation of each component with the seasonal cycle (PC1). For interpretation, this vector points in the direction of where the surface current is intensified (but not necessarily oriented) when PC1 is more positive, but the size of the vector depends on how closely correlated the local velocity is to PC1, rather than the magnitude of the velocity.

3 Physical drivers of reef connectivity variability in the southwest Indian Ocean

3.1 High-frequency variability

Temporal variability in reef source strength across the southwest Indian Ocean is summarised in Figure 2, spanning a wide range of timescales, from days to multiple years. However, the source strength at most reefs simulated by SECoW is dominated by high-frequency variability on the order of days to weeks. As shown by Figure 2(a), a low-pass filter with a threshold of longer than ∼20 days removes most of the variance in daily source strength for the vast majority of reef cells within the southwest Indian Ocean. Although an annual and, in some cases, biannual cycle is detectable at most sites, this variability is only *dominant* at a small minority of sites.

https://doi.org/10.5194/egusphere-2023-778
Preprint. Discussion started: 25 April 2023

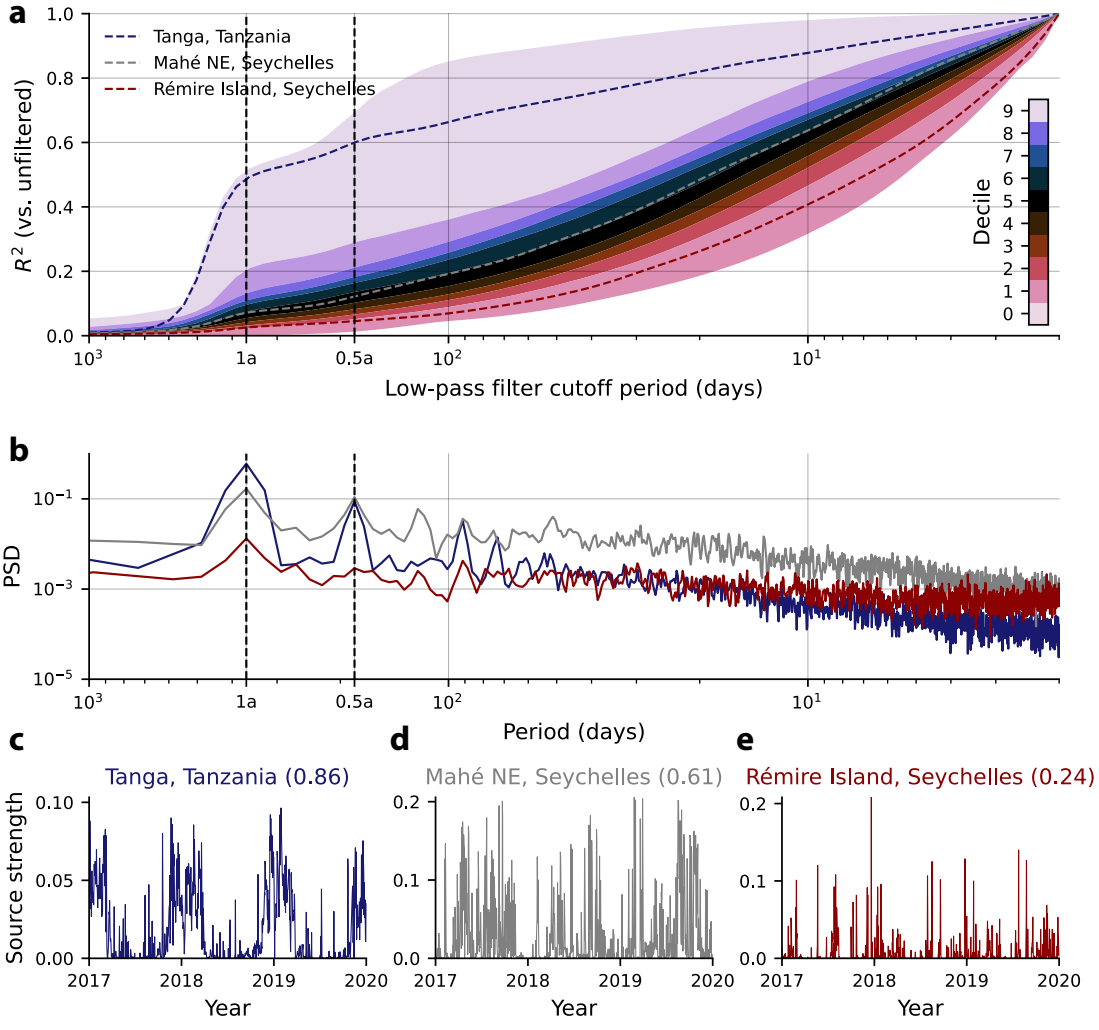

Figure 2. (a) Variance fraction of unfiltered (daily) source strength explained by low-pass filtered source strength, as a function of the low-pass filter cutoff period, expressed as deciles across the 8088 reef cells. Also shown in dashed lines are examples of three particular reef cells, dominated by low frequency variability (Tanga), high-frequency variability (Rémire Island), and a mixture (Mahé). Animations giving further insight into variability at these three sites can be found in Supplementary Animations 1-3. **(b)** Source strength power spectral density for the three example reef cells using Welch's method. **(c-e)** Three years of the full source strength time-series for the three example reef cells. The numbers in brackets in subplot titles refer to the 1 day lagged autocorrelation (see section Section 2.2.1).

165 High-frequency potential connectivity variability (using the 1 day lagged autocorrelation of source strength, r_{1d}, as a proxy, with lower values corresponding to greater high-frequency variability) varies enormously across the southwest Indian Ocean (Figure 3). One clear pattern from this figure is that remote reefs far from land are associated with a greater level of high-frequency potential connectivity variability, such as many of the atolls belonging to the Amirante Islands in Seychelles (Fig-

https://doi.org/10.5194/egusphere-2023-778
Preprint. Discussion started: 25 April 2023

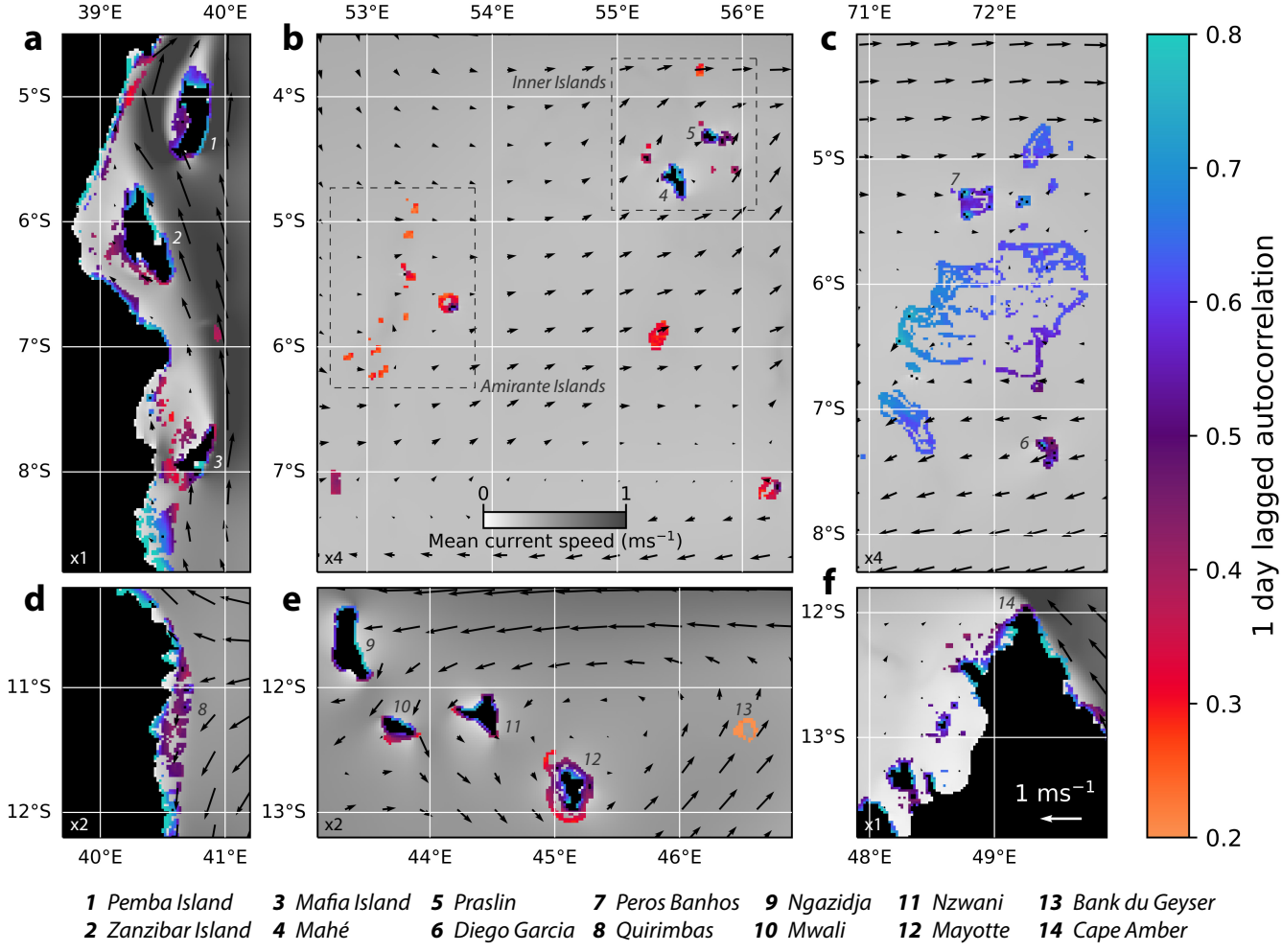

Figure 3. 1 day lagged autocorrelation, r_{1d}, for the source strength time-series of individual reef cells. The corresponding figure for the full domain is provided in the supplementary materials but, for clarity, this figure focuses on 6 sub-regions: (a) north Tanzania; (b) Seychelles, excluding the Aldabra and Farquhar Groups; (c) the Chagos Archipelago; (d) the Quirimbas Archipelago, Mozambique; (e) the Comoro Islands, including Banc du Geyser; and (f) north Madagascar. Background shading represents the mean current speed, with arrows representing the mean current velocity. For clarity, arrows are enlarged relative to the scale in panel (f) by the scale-factor indicated in the lower-left corner of each sub-plot.

ure 3(b), west) and Bank du Geyser (Figure 3(e), east). The geographic remoteness reduces the probability that larvae spawning from these sites will be above a reef during its competency window, and the lack of nearby land allows larvae to pass over reefs without getting trapped against the coast, reducing the time spent above a reef environment. As a result, source strength from these remote reefs is highly inconsistent and driven by short-lived settling pulses. A similar effect is seen at reefs further away

https://doi.org/10.5194/egusphere-2023-778
Preprint. Discussion started: 25 April 2023

from land along the Quirimbas Archipelago in Mozambique (Figure 3(d)). Although some particularly remote reefs such as Bassas da India in the south Mozambique Channel (Supplementary Animation 4) and St. Brandon in Mauritius have a relatively high source strength autocorrelation (Supplementary Figure 2), this is because these sites are so remote that the source strength is zero for many days, inflating the r_{1d} statistic. Highly variable and sporadic source strength is therefore a robust characteristic of small and remote reefs in SECoW.

For some islands, the orientation of the coastline relative to prevailing ocean currents drives r_{1d}. The east and north coasts of Ngazidja and Mwali (Comoros, Figure 3(e)) face surface currents entering the Mozambique Channel, thereby trapping larvae against the coast and resulting in consistent settling. For instance, practically all larvae spawning from the east coast of Ngazidja settle at reefs along the same coastline, whereas a greater proportion of larvae spawning from the opposite side of Ngazidja settle at other islands (which are lower-probability connections, and hence subject to greater variability). The interaction of ocean currents with the coastline, as previously described in depth by Mayorga-Adame et al. (2016, 2017) is also important in setting r_{1d} along the path of the East Africa Coastal Current (EACC, Figure 3(a)). Larvae spawning from reefs around Chole Bay on the southeast coast of Mafia Island (by the '3' label in Figure 3(a)) get trapped within the bay and are therefore less likely to enter the EACC. Entering the EACC results in longer distance transport and less reliable connections, so larval retention around Chole Bay results in higher r_{1d}. In contrast, larvae spawning from reefs in the west and northeast of the island are very likely to enter the EACC, and therefore have a much lower r_{1d}.

A complex set of flow reversals and wake eddies are generated as the EACC is diverted by headlands and islands, resulting in highly localised connectivity regimes. For instance, similarly to the numerical model described in Mayorga-Adame et al. (2016), flow reversals are generated around Zanzibar Island and Pemba Island (Supplementary Figure 3). Flow is weakened in the wake of a peninsula on the east coast of Zanzibar, trapping larvae near their source reefs, occasionally exacerbated by convergent flow towards the coast. A similar effect is seen off the north tip off Pemba Island, where flow is slower in the wake of the island and is often oriented towards the coastline. Conversely, west of Pemba Island, currents are often seaward (perhaps associated with localised upwelling described by Painter et al. (2021)), enabling larvae to drift away from the coast and enter the EACC, again facilitating longer distance, less reliable connections. Similar explanations account for the pattern of high-frequency source strength variability in northernmost Madagascar (Figure 3(f)). Larvae spawning east of Cape Amber (the north cape of Madagascar) are trapped against the coast by the Northeast Madagascar Current (NEMC) and are therefore associated with high r_{1d}. Larvae spawning from Cape Amber itself are catapulted into the NEMC and are correspondingly subject to much greater source strength variability.

In the Chagos Archipelago (Figure 3(c)), due to the general lack of exposed land and enormous reef area, the drivers of source strength variability are quite different. Here, source strength variability is lower in areas of more concentrated reef cover. Where there is less nearby reef area (such as the southwest rim of the Grand Chagos Bank), connections are less likely and consistent, resulting in higher day-to-day source strength variability, and therefore lower r_{1d}.

Figure 4 shows that, for much of the southwest Indian Ocean, a large proportion of this variability can also be *quantitatively* explained by several key metrics. For the EACC and islands in the path of the NEMC (Figure 4(a, d)), the weighted connection distance (i.e. the weighted mean distance from a reef cell to downstream settlement reefs) explains around half of the variance

https://doi.org/10.5194/egusphere-2023-778
Preprint. Discussion started: 25 April 2023

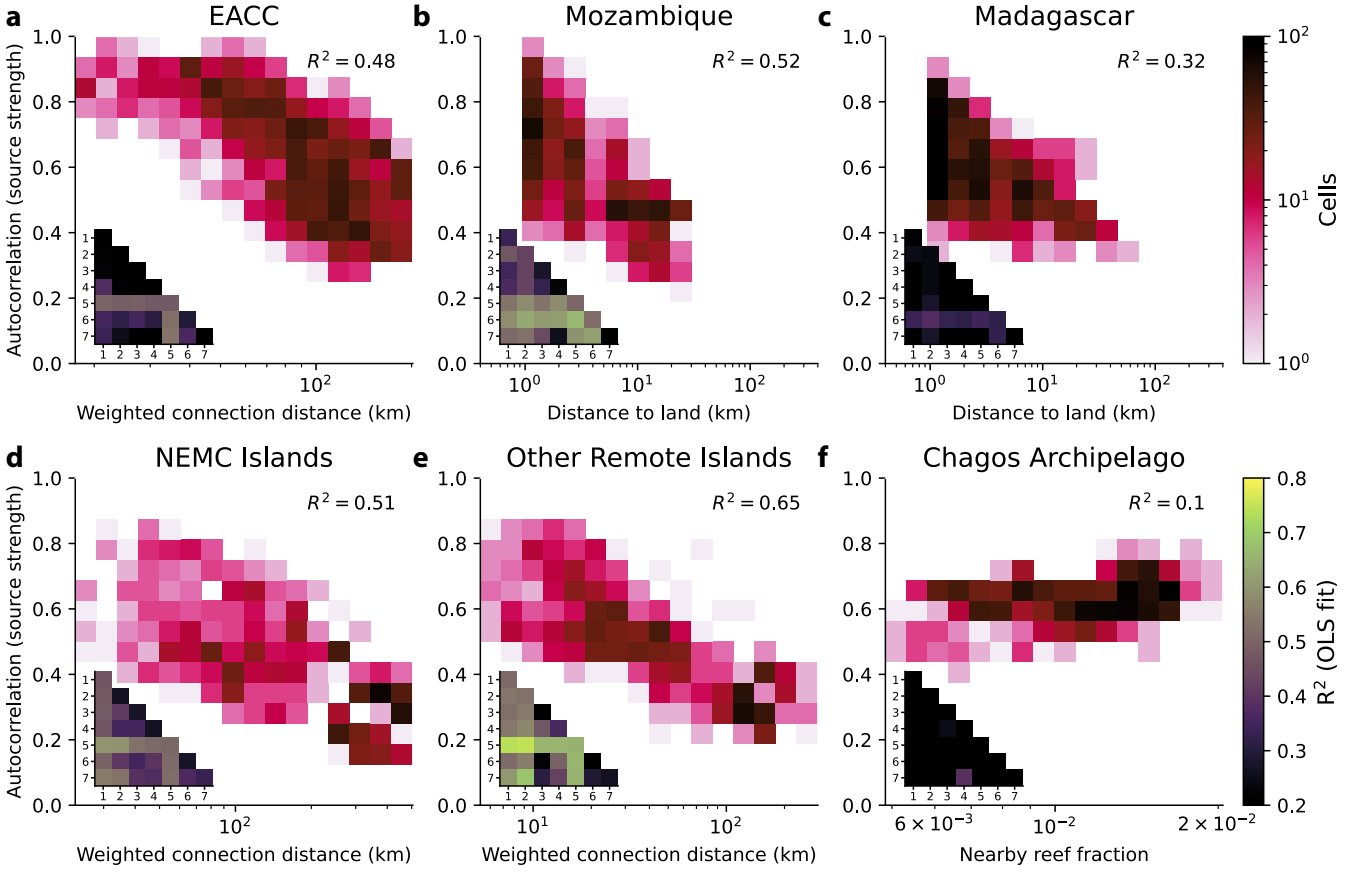

Figure 4. Histograms for the 1 day lagged autocorrelation of source strength for individual reef cells, as a function of a predictor variable. The predictor variable plotted is the variable with the highest R^2 value from ordinary least-squares regression with the source strength autocorrelation. The matrices in the lower-left corner of each sub-plot represent the R^2 value from ordinary least-squares regression based on all *pairs* of predictor variables, namely (1) Mean current speed; (2) Mean high-frequency current speed; (3) Mean sub-daily current speed; (4) nearby reef fraction; (5) weighted connection distance; (6) Distance to land; and (7) Mean source strength.

in r_{1d}. For other remote islands (Figure 4(e)), this rises to almost two thirds. Larvae in these settings tend to travel greater distances (due to a combination of current speed and/or relatively few nearby reefs) so the proximity of downstream reefs is a strong predictor of day-to-day potential connectivity variability. Reefs where the dominant larval destinations are within tens of kilometres tend to have less high-frequency potential connectivity variability. Unfortunately, weighted connection distance is a less-generalisable metric for decision making, as this cannot be easily measured without running a larval dispersal model. For the EACC, weighted connection distance was the only metric acting as a reasonable predictor for r_{1d}. However, as can be seen in the insets in Figure 4, there was a significant (negative) correlation between the local mean current speed and r_{1d} for NEMC islands ($R^2 = 0.47$) and other remote islands ($R^2 = 0.51$). The high-frequency current speed (associated with

https://doi.org/10.5194/egusphere-2023-778
Preprint. Discussion started: 25 April 2023

current variability in the 1-30 day range) was also strongly negatively correlated with r_{1d} for other remote islands ($R^2 = 0.53$). Therefore, the local current speed near remote island reefs may be a reasonable first-order predictor of the magnitude of high-frequency potential connectivity variability. The simple explanation is that greater current speeds are more likely to transport larvae away from the remote island, and into the open ocean where chances for settlement will be rare and sporadic.

For reefs along the coasts of Mozambique and Madagascar, the distance to land was generally the strongest explanatory variable for r_{1d}. In the case of Mozambique, this pattern is driven by the Quirimbas Archipelago (Figure 3(d)), but several other explanatory variables also perform similarly well, namely the weighted connection distance ($R^2 = 0.50$) and the high-frequency current speed ($R^2 = 0.43$). For Madagascar, none of the predictor variables were particularly strong, and this may be due to the highly complex coastline and multiple oceanographic regimes (the eddy-dominated Mozambique Channel in the west, and the North and Southeast Madagascar Currents in the north and east).

Finally, high-frequency potential connectivity variability at the Chagos Archipelago is only weakly correlated with any of the explanatory variables we tested. As hinted at by the general increase in variability towards parts of the Grand Chagos Bank with lower reef cover, there is weak positive correlation between nearby reef fraction and r_{1d}. However, with minor exceptions, r_{1d} does not vary by much across the archipelago, with moderate-to-high r_{1d} across most reefs (Figure 3).

For most regions, pairs of predictor variables lead to a slight, but not major, improvement in r_{1d} (Figure 4 insets). The only very substantial improvement is for the Chagos Archipelago, where adding the time-mean source strength to nearby reef fraction in the OLS regression model almost quadruples the R^2 value to 0.39. A high time-mean source strength is indicative of many consistent nearby connections, although as with the weighted connection distance, this metric cannot be easily estimated without running a dispersal model.

In summary, a first-order rule of thumb for estimating high-frequency potential connectivity variability is as follows. For reefs at remote atolls lacking substantial land, r_{1d} is likely to be very low (with highly sporadic and pulsed source strength). For reefs associated with substantial islands that are nonetheless remote, the local current speed (and potentially the component associated with variability on timescales of less than a month) may be a reasonable indicator of r_{1d}, with higher local current speeds associated with less reliable potential connectivity. For reefs near continental coasts, predicting potential connectivity variability without a larval dispersal model is likely to be challenging, although consideration of local geography and ocean dynamics may be helpful. For instance, potential connectivity variability will likely be greater for reefs further from the coast. Consideration of whether local ocean currents hinder or facilitate long-distance dispersal may also provide insights into potential connectivity variability as, the more likely long-distance dispersal is, the less reliable connectivity is likely to be. Finally, for exceptional regions of extensive reef cover such as the Chagos Archipelago, potential connectivity variability will generally be lower, but may increase in isolated sectors with lower reef cover. The exact ranking of predictors varies slightly based on biological parameters (Supplementary Table 2), but the rule of thumb above is rather robust.

3.2 Seasonal variability

Once high-frequency variability is removed from the source strength time-series for each cell by computing monthly means, the dominant residual signal is the seasonal cycle. The regular (mean) seasonal cycle explains a median of 25.6% of the variance

https://doi.org/10.5194/egusphere-2023-778
Preprint. Discussion started: 25 April 2023

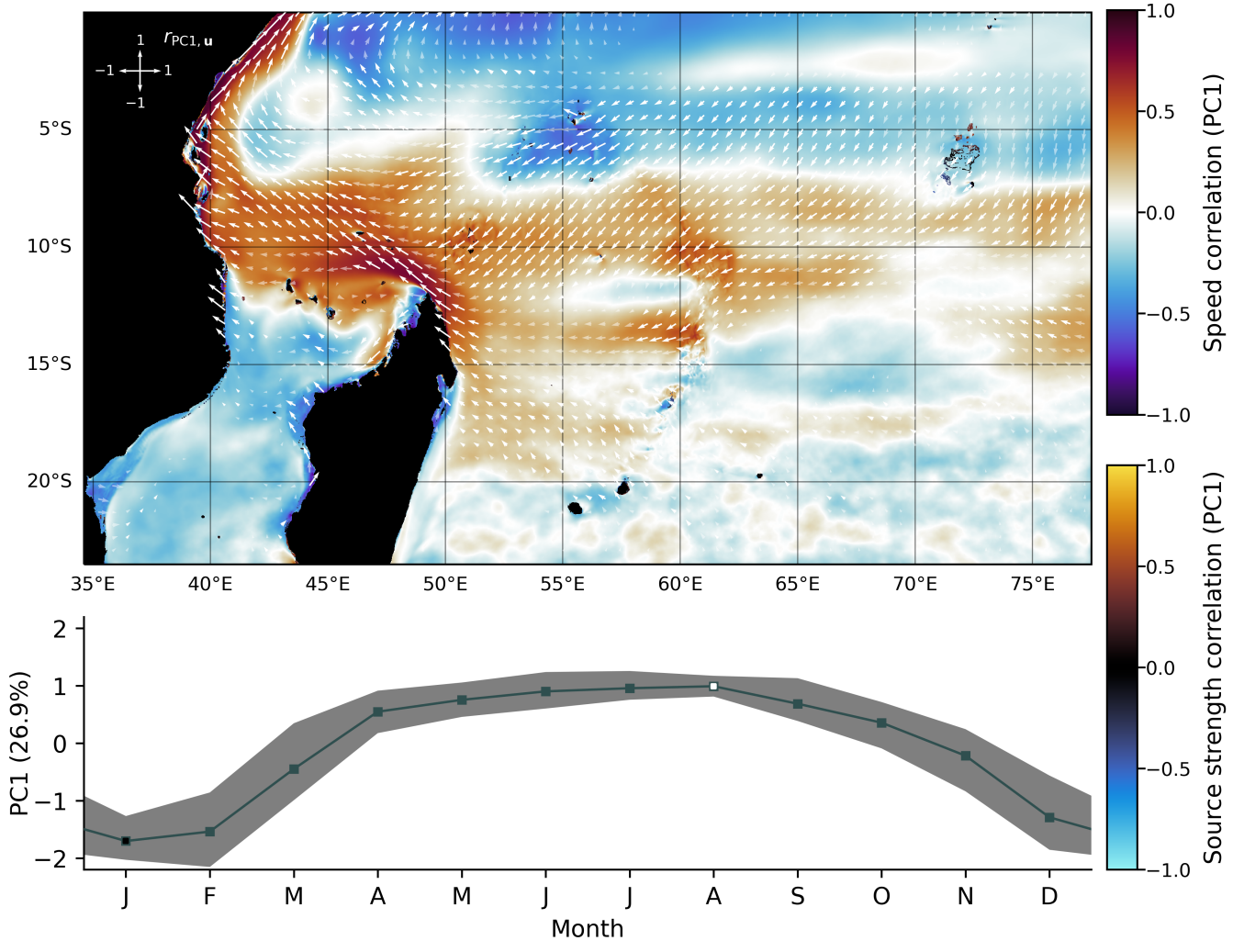

Figure 5. Background colours represent the correlation of ocean current monthly mean speed with PC1 (from the source strength matrix). The correlation of monthly mean source strength with PC1 is also shown, but please see Figure 6 for enlarged views. *Inset:* Seasonal cycle of PC1 computed as the monthly climatology, with the total range for monthly means across all years (1993-2019) shaded.

in monthly mean source strength across reef cells, rising to 65.0% for reefs under the influence of the EACC. Since seasonal variability across much of the southwest Indian Ocean is driven by the monsoons, much of this variability is broadly in phase. Decomposing the monthly-mean source strength matrix into a set of Empirical Orthogonal Functions, we unsurprisingly find that the dominant EOF corresponds to the seasonal monsoonal cycle (PC1, Figure 5), switching sign between the northwest monsoon (broadly December to February) and southeast monsoon (broadly June to August). PC1 explains 26.9% of the variance in monthly mean source strength, more than double that of the next principal component (Supplementary Figure 4), and

https://doi.org/10.5194/egusphere-2023-778
Preprint. Discussion started: 25 April 2023

is very stable, with only minor interannual variation. PC1 is strongly linked to the strength of the EACC and NEMC, as well as to the position and strength of the South Equatorial Current (SEC) and South Equatorial Countercurrent (SECC) (e.g. Swallow et al., 1991; Schott et al., 2009; Yamagami and Tozuka, 2015; Manyilizu et al., 2016; Aguiar-González et al., 2016; Painter, 2020). In addition to current strength, current direction is strongly correlated with PC1, most notably for reefs in Somalia, Seychelles and the Chagos Archipelago.

In many cases, seasonal variability in current speed and source strength are anticorrelated. For instance, the source strength for most reefs along the path of the EACC is suppressed when the current is at its strongest (e.g. Figure 6(a) - note how source strength across most reefs is negatively correlated with PC1, and therefore the strength of the EACC, see also Figure 5). Although faster currents tend to facilitate long-distance connections, due to the effects of mortality, dispersion and competency loss, these connections are practically always weaker than the short-distance connections that are simultaneously suppressed. Some local exceptions exist, such as in the west Zanzibar Channel, where stronger northward flow during the southeast monsoon facilitates the flow of larvae towards higher reef cover in the north. However, in general, this pattern is very robust along the Tanzanian and Kenyan coasts, as well as across most islands directly in the path of the NEMC (such as the Aldabra and Farquhar Groups of Seychelles), and reefs at the north tip of Madagascar. Current speed also appears to be primarily responsible for the seasonal variability in the Comoro Islands (Figure 6(e)). Flow here is highly complex due to strong eddy activity, but generally faster flow during the southeast monsoon results in lower retention within each island, and therefore lower source strength. This pattern reverses at the south of each island, possibly due to flow reversals and current weakening in the island wakes.

At other locations, seasonal variations in current *direction* appear to have a greater influence on source strength variability. This is clearest at the Chagos Archipelago (Figure 6(e)), where southwestward currents suppress source strength in the southwest of the Archipelago during the southeast monsoon. For these marginal atolls, southwestward larval transport sends larvae directly into the open ocean, resulting in almost inevitable death. It is, however, important to note that correlation with PC1 is generally quite weak across the Chagos Archipelago. On Mahé in Seychelles, the seasonal cycle in source strength is in antiphase for the south and north halves of the island (Figure 6(b)). In the south, weaker currents during the southeast monsoon result in strong larval retention within Mahé (and therefore higher source strength). However, a westward component to currents affecting the north of the island results in larval transport away from Mahé, locally reducing source strength. These patterns are reversed during the northwest monsoon. A similar effect occurs on the nearby island of Praslin.

Although the intensification of the NEMC during the southeast monsoon explains the anticorrelation of source strength with PC1 in northernmost Madagascar, this anticorrelation continues along ocean-facing reefs across much of the northwest coast. Here, an off-shore component to currents along the coast develops during the southeast monsoon, transporting larvae off the Madagascan shelf. An energetic mesoscale eddy field within the Mozambique Channel rapidly transports larvae away from Madagascar once they leave the shelf, resulting in low source strength during the southeast monsoon (compare high retention during the northwest monsoon in Supplementary Animation 5, to low retention during the southeast monsoon in Supplementary Animation 6). A similar seasonal switch in the cross-shore flow component is responsible for antiphase seasonal correlations in source strength across the Quirimbas Archipelago in Mozambique (Figure 6(d)). The cross-shore component

https://doi.org/10.5194/egusphere-2023-778
Preprint. Discussion started: 25 April 2023

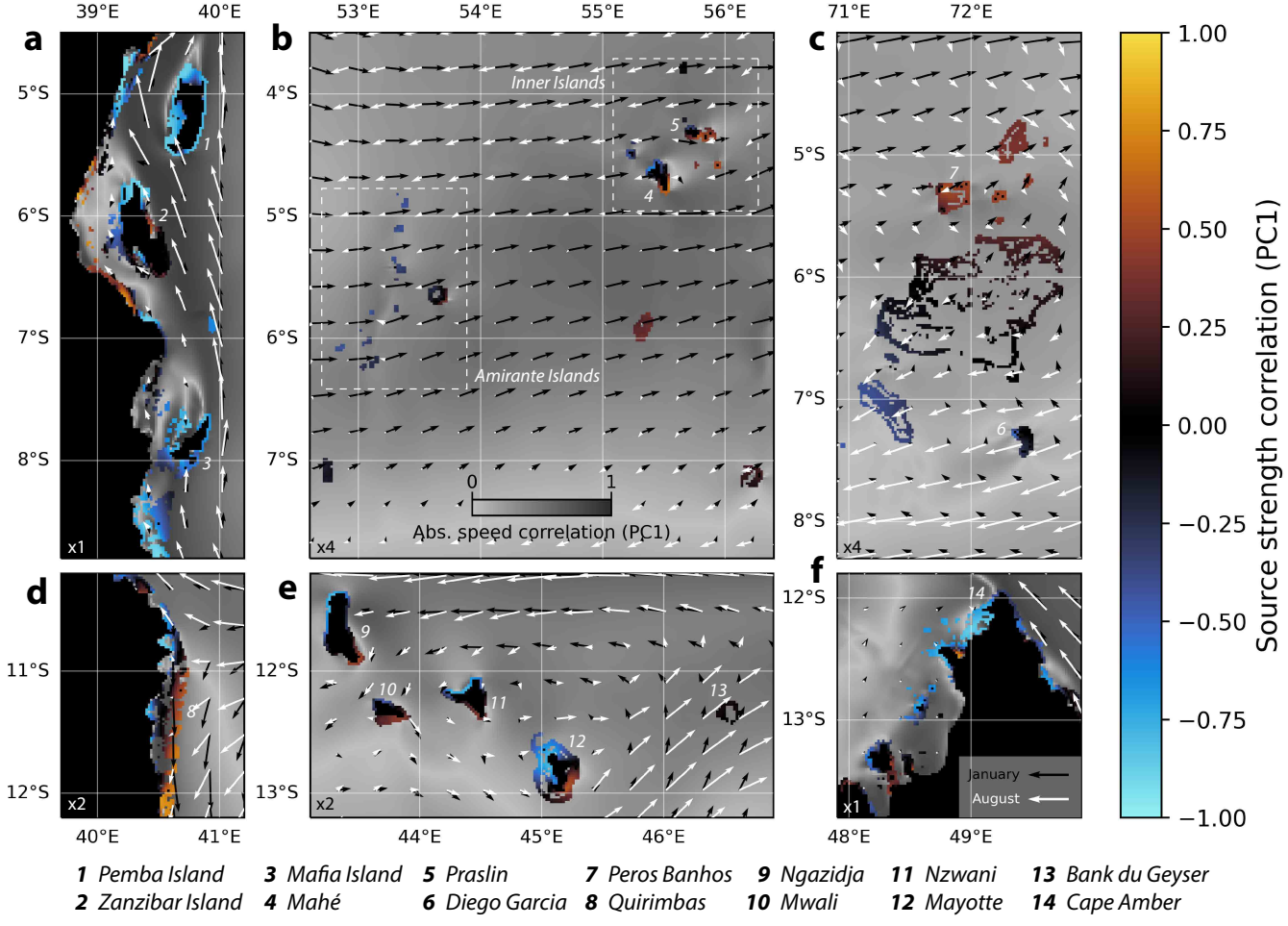

Figure 6. Close-up views of selected reefs from Figure 5: (a) north Tanzania; (b) Seychelles, excluding the Aldabra and Farquhar Groups; (c) the Chagos Archipelago; (d) the Quirimbas Archipelago, Mozambique; (e) the Comoro Islands, including Banc du Geyser; and (f) north Madagascar. Colours represent the correlation of monthly mean source strength with PC1. The background is shaded by the correlation between ocean current monthly mean speed and PC1 as in Figure 5 but, for clarity, we show the magnitude only, in greyscale. Arrows show mean current velocities during minimum (January [northwest monsoon], black) and maximum (August [southeast monsoon], white) PC1.

is oriented towards the coast during the southeast monsoon, preventing larvae from the outermost reefs from being lost into the Mozambique Channel, thereby increasing their source strength. Conversely, the weakening of these cross-shore currents during the northwest monsoon allows larvae from reefs nearest to the coast to disperse towards the higher reef cover at the outer reefs, whilst larvae from the outer reefs are more likely to be lost to the open ocean.

In general, SECoW suggests that seasonal variability in source strength is strong and largely synchronous, if spatially heterogeneous, along the path of the EACC. This is also true for the NEMC but to a lesser extent, due to the lack of continuous

https://doi.org/10.5194/egusphere-2023-778
Preprint. Discussion started: 25 April 2023

reef along this current. PC2 is an annual cycle (like PC1) but lagged by around 3 months, and may represent local phase shift in the seasonal cycle. When PC2 is positive, flow strengthens in the Mozambique Channel, weakens within the EACC core, and the SEC shifts towards the north (Supplementary Figure 5). At a small number of reefs, such as the east coast of Zanzibar, PC2 is more strongly correlated with source strength than PC1 (Supplementary Figure 6). Although PC2 accounts for only 11.7% of the variance in monthly mean source strength across the domain, it has greater interannual variability than PC1, with PC2 anomalies being associated with strengthened southeasterly winds over the tropical, westernmost Indian Ocean. PC1 and PC2 are the dominant modes of seasonal variability, with remaining principal components generally associated with local current variability. Although interannual variability is generally small compared to high-frequency variability (Figure 2(a)), it can be locally significant compared to seasonal variability outside of the EACC and NEMC, and is largely stochastic (driven by mesoscale ocean variability) rather than being explained by large-scale and synchronous changes in winds and ocean currents. Although climate modes such as the Indian Ocean Dipole (IOD) are associated with zonal current variability in the Indian Ocean (Schott et al., 2009; Nagura and McPhaden, 2010; Sachidanandan et al., 2017), any effect on potential connectivity in our simulation is negligible compared to seasonality and stochastic variability.

3.3 Limitations

Although our simulations account simplistically for biological processes such as mortality, competency acquisition and loss, and settling rates depending on available reef cover, we do not incorporate environmental influences on coral larval mortality and competency, such as temperature (Nozawa and Harrison, 2007; Figueiredo et al., 2022). For instance, during IOD events, the temperature of the upper ocean rises in the west Indian Ocean. Although we found no significant effect of the IOD on potential connectivity in SECoW, it is possible that realised dispersal is nevertheless suppressed during IOD events due to the increased larval mortality rate. On the other hand, IOD events are generally most strongly expressed in the west Indian Ocean during October to November, which only partially overlaps with the general spawning season in the region (Mangubhai and Harrison, 2009; Koester et al., 2021; Baird et al., 2021). In addition to interannual temperature variability, temperature also varies over shorter timeframes and spatial scales, from meso- to frontal. This high-frequency temperature variability could add a further stochastic component to dispersal, particularly if a dense larval filament were subjected to protracted high or low temperatures by entrapment in an eddy or front. Including a dependence of larval mortality to temperature would add yet another degree of freedom to our larval biological parameterisation, so we do not investigate this in the present study. However, daily surface temperature is available within WINDS (Vogt-Vincent and Johnson, 2023), so this could be included in a future dispersal model.

Although WINDS is the highest resolution ocean model that has been run on such large spatial and temporal scales in the southwest Indian Ocean, the approximately 2km resolution is still insufficient to resolve flow on a reef scale. As a result, although we expect SECoW to reasonably simulate larval dispersal within the open ocean, larval retention may be overestimated by our simulations along continental coastlines (Dauhajre et al., 2019), and underestimated around atolls (Grimaldi et al., 2022). Given that long-distance connections are associated with greater high-frequency potential connectivity variability (Section 3.1), our study may underestimate source strength variability for reefs across East Africa and Madagascar. Conversely,

https://doi.org/10.5194/egusphere-2023-778
Preprint. Discussion started: 25 April 2023

it is likely that our study overestimates potential connectivity variability for larvae originating from remote coral atolls. The highest frequency of variability we consider in this study is 1 d^{-1}. Larval dispersal will vary at even higher frequencies, for instance following tidal cycles (Green et al., 2018; Grimaldi et al., 2022). However, although particles in SECoW do experience tides, which are reproduced well by WINDS over the open ocean (Vogt-Vincent and Johnson, 2023), complex, reef-scale interactions between tides, waves, and reef geomorphology will not be reasonably represented. We therefore do not investigate the variability of larval dispersal with respect to tidal phase.

By considering total reef area, SECoW certainly overestimates the distribution of any one particular coral species, and furter assumes that coral fecundity is constant. These assumptions are necessary due to the lack of data in the southwest Indian Ocean, but they are nevertheless important limitations. Insofar as potential connectivity variability is concerned, temporal variability in fecundity, both stochastic and as a response to environmental stress (Levitan et al., 2014; Pratchett et al., 2019; Hartmann et al., 2018; Leinbach et al., 2021; Nakamura et al., 2022), may be particularly important. Again, it is not clear to what extent this may amplify or dampen connectivity variability induced by ocean currents.

4 Consequences for demographic and genetic connectivity studies

4.1 'Interannual' variability for short spawning events is dominated by high-frequency variability

The importance of interannual variability for potential connectivity is recognised by some modelling studies. For instance, Thompson et al. (2018) investigated potential connectivity in the Coral Triangle using a 47-year hindcast, and found that at least 20 years of simulated spawning events were required to reasonably represent interannual connectivity variability. This is concerning, as many (if not most) larval dispersal modelling studies continue to use considerably shorter timespans. What was not clear, however, is whether this variability in potential connectivity between annual spawning events reflected genuine low frequency (interannual) oceanographic variability, or whether this simply reflects underlying high frequency variability in surface currents.

To test this, we compute the coefficient of variation (CV) for source strength and flux (i.e. the standard deviation divided by the mean) as a function of the number of spawning events, for five different types of spawning behaviour: (1) a 1-day annual spawning event, (2) a 5-day annual spawning event, (3) a month-long annual spawning event, (4) year-round spawning, and (5) a 1-day spawning event every 10 days. Time-series 1-4 have a total length of 27 years, and time-series 5 has a total length of 270 days (i.e. all have 27 spawning events). For each time-series, we compute the median CV, and 5^{th} - 95^{th} percentile range, across all reef cells or connections. To eliminate biases associated with a particular season or year, we compute 12 different time-series for scenarios 1-3 (one for each spawning month) and scenario 5 (one for each year from 2008-2019), and average across them. Since many individual connections in the flux matrix are below the detection threshold of SECoW, we excluded all connections which are always zero.

The solid black line in Figure 7 shows how the CV of (a) source strength and (b) flux for an annual 1-day spawning event increases with the number of spawning events (years). Despite representing an entirely different region, Figure 7(b) shows a strong resemblance to the results of Thompson et al. (2018), with several decades of data (tens of spawning events) required

https://doi.org/10.5194/egusphere-2023-778
Preprint. Discussion started: 25 April 2023

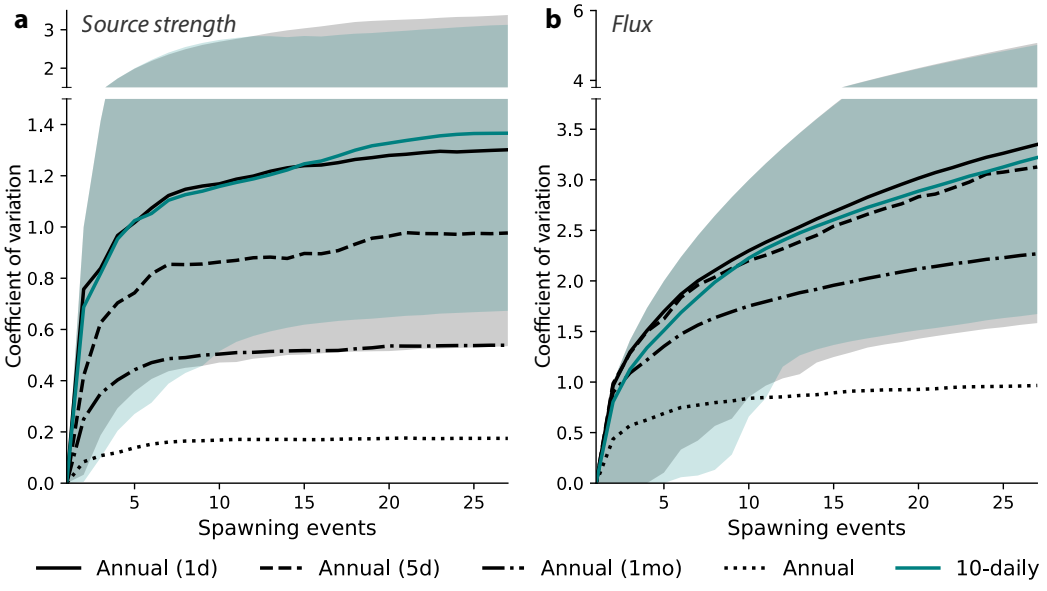

Figure 7. (a) Source strength CV across reef cells with a significant detectable source strength in SECoW for (*black*) annual spawning events from 1993-2019, assuming spawning takes place over (solid) 1 day, (dashed) 5 days, (dash-dotted) 1 month, and (dotted) continuously on an annual basis; and (*teal*) spawning events lasting one day every 10 days. The shaded area represents the 5^{th} - 95^{th} percentiles for the annual 1 day spawning events (black) and 10-daily spawning events (teal). (b) As with *(a)*, but for flux (based on groups, not cells). Note the different y scale.

to adequately characterise the variability associated with potential connectivity between reefs. In contrast to flux, interannual variability in source strength (Figure 7(a)) can be reasonably represented by only around ten years of data. In addition to reaching a plateau more quickly, the magnitude of the CV is generally significantly smaller for source strength than flux. Source strength is proportional to the integral of flux across all sink cells, so it is unsurprising that this metric is less variable than flux, despite flux being computed here using groups rather than cells.

If interannual variability in potential connectivity were driven by interannual oceanographic variability, we would not expect the CV to be sensitive to spawning duration (below a year). However, for source strength, the interannual variability falls rapidly with increased spawning event duration. For instance, increasing the spawning event duration from 1 day to 5 days reduces the CV by about a third. This demonstrates that protracted spawning, even as little as a few days, is an effective method of improving source strength stability (i.e. the likelihood of larvae settling anywhere). In contrast, the source strength CV for year-round spawning is typically around 0.2 for many reefs (Figure 7(a)), indicating that the mean source strength over a year only varies slightly from the longer-term average. A qualitatively similar pattern is seen for flux, although the CV for 5-day spawning events is similar to 1-day spawning events (likely due to the highly transient nature of individual reef-reef connections).

https://doi.org/10.5194/egusphere-2023-778
Preprint. Discussion started: 25 April 2023

The teal line in Figure 7 shows the CV for source strength (a) and flux (b) for a simulated 1-day spawning event occurring every 10 days, rather than every year. Despite the fact that this time-series captures zero interannual variability and is based on a biologically unrealistic spawning scenario, the median CV is practically indistinguishable between 1-day spawning events every 10 days versus every year. This strongly suggests that, to first-order, interannual dispersal variability for short spawning events reflects stochastic high-frequency oceanographic variability, rather than being driven by genuine interannual oceanographic variability. The source strength variance for single day spawning events separated by 10 days versus a year begin to diverge slightly after around 15 spawning events. For spawning events separated by 10 days, this corresponds to a total duration of 150 days, which is sufficient time to switch between opposite monsoon phases (introducing additional variance due to seasonal variability). However, this is unlikely to be relevant for most corals, as few broadcast spawning corals spawn across different phases of the monsoonal cycle.

To summarise, although there is genuine interannual variability in the source strength and flux time-series (reflecting the underlying oceanographic forcing, see Vogt-Vincent and Johnson (2023)), most variation in potential connectivity across annual spawning events is simply an artefact arising from low-frequency sampling of a signal dominated by high frequency variability.

4.2 Most settling larvae are generated by a small minority of spawning events

Although protracted spawning periods have been observed or inferred for some broadcast-spawning corals in the west Indian ocean (e.g. Mangubhai and Harrison, 2008; Sola et al., 2015), spawning is often short and synchronous, taking place over a few nights per year at most (e.g. Mangubhai et al., 2007; Bronstein and Loya, 2011; Sola et al., 2016). Since source strength is generally dominated by day-to-day variability (Section 3.1), the fate of coral larvae generated by a spawning event is very sensitive to exact timing of spawning.

As described in Section 4.1, source strength variability for short spawning events is dominated by stochastic high-frequency variability. Since the autocorrelation timescale[1] is less than 10 days for almost all reefs in SECoW (the 99^{th} percentile is 9.9 days), we can approximate 1-day spawning events separated by 10 days as being independent. We thereby generated a synthetic multi-centennial source strength time-series by imagining a coral species that spawns one day per year, and extracting the source strength at each reef site every 10 days between December to February (within the general spawning period for broadcasting corals in the southwest Indian Ocean (Mangubhai and Harrison, 2008; Mangubhai, 2009; Koester et al., 2021; Baird et al., 2021)) from 1993-2019. This resulted in a time-series spanning 243 (9×27) spawning events (or years). From this time-series, we computed the smallest proportion of events that account for 50% of all successfully settling larvae. Finally, we repeated this process ten times to cover all simulated spawning events in December to February, and averaged across these ten initialisations.

SECoW predicts that half of all settling larvae were generated by only 13.3% of annual spawning events (the median across all reef cells). However, this falls to below 4.0% for the decile of reefs with the greatest source strength variability and, for 47 reefs, this figure was less than 1%. In other words, for these reef sites, most settling larvae were generated by a once-in-a-century spawning event. Reefs with the most unequal temporal distribution of source strength were almost always

[1]Computed based on $r_{1\text{d}}$ assuming $r = \exp(-t/\tau)$, where τ is the autocorrelation timescale.

https://doi.org/10.5194/egusphere-2023-778
Preprint. Discussion started: 25 April 2023

remote islands, including most of Seychelles, isolated reefs in Mozambique and Madagascar, Réunion, and the Outer Islands of Mauritius (Figure 8). The reefs with the most consistent year-to-year source strength were mostly along the path of the EACC, due to the relatively continuous reef along the coast and predictable, consistent ocean currents.

Some corals have been observed to 'split spawn', i.e. undergo multiple spawning events within a reproductive season, often (but not always) separated by a month (Willis et al., 1985; Bastidas et al., 2005; Foster et al., 2018). A previous modelling study based on the Great Barrier Reef found that split spawning separated by a month can significantly increase the reliability of larval supply (Hock et al. (2019), with similar results also found by Kough and Paris (2015). Our finding that a minority of spawning events generate most settling larvae supports this finding (in a very different and diverse oceanographic context), as a greater number of individual spawning events significantly increases the likelihood of a rare 'high-impact' dispersal event.

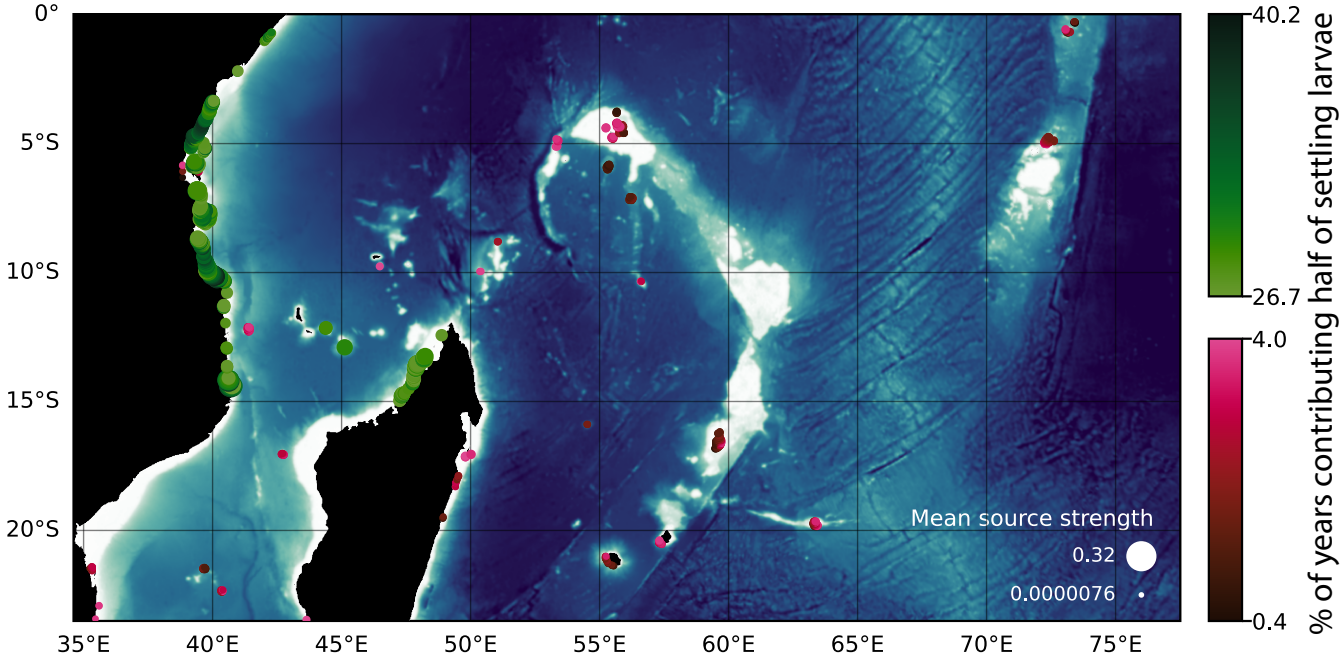

Figure 8. Percentage of years contributing half of successfully settling larvae (colours), shown for the lowest and highest decile of reef cells only. Markers are scaled by the mean source strength, and do not represent the physical size of reef cells.

4.3 High-frequency oceanographic variability introduces considerable uncertainty to connectivity predictions

Dispersal variability significantly affects metapopulation dynamics (Watson et al., 2012), but this is neglected by many modelling studies, which generally only publish a time-mean potential connectivity matrix. Time-mean potential connectivity matrices are also widely used to explain genetic connectivity (e.g. Foster et al., 2012; Padrón et al., 2018; Horoiwa et al., 2022), and to explore long-term population persistence and eco-evolutionary dynamics (e.g. Kleypas et al., 2016; McManus

https://doi.org/10.5194/egusphere-2023-778
Preprint. Discussion started: 25 April 2023

et al., 2021; Holstein et al., 2022). However, given the enormous variability in potential connectivity, it is pertinent to consider the uncertainty oceanographic variability may introduce into these predictions.

For this purpose, we consider the backward *cumulated multistep implicit connectivity*, hereon CMIC for brevity, defined by Ser-Giacomi et al. (2021). For a pair of nodes (reef groups) i and j, the CMIC for n steps gives the probability that a pair of random walks terminating at i and j passed through the same node within n steps. If post-settlement processes are neglected and steps of a random walk are interpreted as gene flow, the CMIC may reflect the degree of shared ancestry for a pair of reefs over a given number of generations (Legrand et al., 2022), with 1 indicating definite shared ancestry, and 0 indicating zero shared ancestry. We compute the CMIC between all pairs of reef groups across 100 steps, randomly sampling potential connectivity matrices assuming spawning events occur across one day during the northwest monsoon. We repeat this process 1000 times, to generate a large set of possible dispersal histories, sampling across the range of primarily stochastic oceanographic variability.

This is shown in Figure 9 for 100 randomly chosen pairs of sites. The CMIC computed from the time-mean flux matrix (black points in Figure 9) is rarely close to the median CMIC (white points) across the 1000 realisations, and ordering CMIC using the time-mean flux matrix would result in a completely different ranking to most CMIC estimates based on time-varying flux matrices. For weaker connections (separated by more dispersal steps), the time-mean CMIC is generally lower than the median CMIC. This suggests that the pulsed nature of connectivity may play an important role in connecting distant populations, which is not adequately represented with the time-mean potential connectivity matrix. Even though we compute the CMIC over a significant number of steps (100), the 5^{th}-95^{th} percentile CMIC range (teal bars) is considerable. This uncertainty is fundamentally related to the stochasticity of ocean currents, thereby imposing limitations on what we can infer about genetic connectivity between site pairs from physical larval dispersal (before even considering uncertainty in biological parameters).

For example, based on the time-mean potential connectivity matrix, high CMIC (and therefore low genetic differentiation) would be expected for the pair of sites marked with an asterisk (*) in Figure 9. If the genetic differentiation between these sites were in fact observed to be high, this could be interpreted as overprinting of the physical connectivity signal by, for instance, selection. This may be correct but, as is clear from Figure 9, high genetic differentiation is, in fact, entirely consistent with the CMIC uncertainty introduced by oceanographic variability. It is therefore not clear how much insight can be gained by, for instance, tuning biophysical models to best fit observed genetic differentiation (Legrand et al., 2022), particularly when CMIC uncertainty can span orders of magnitude when computed over fewer steps (Supplementary Figure 9).

For demographic connectivity (for example, considering the role larval dispersal may play in driving recovery after mass-mortality events), the larval flux over a smaller number of spawning events is more relevant than the CMIC. Summed over a ten-year period, the total number of larvae transported between pairs of sites may vary over several orders of magnitude due to stochastic ocean variability (Supplementary Figure 10), again introducing fundamental uncertainty to what we can predict about demographic connectivity. For instance, the importance for coral resilience of a particular reef-reef connection associated with high time-mean larval flux may be overestimated if that connection has a reasonable chance of being insignificant for a decade or longer. We therefore argue that studies generating potential connectivity data to inform marine management efforts should discuss (and publish) data on dispersal *variability* rather than just the time-mean dispersal matrix (or the mean seasonal

https://doi.org/10.5194/egusphere-2023-778
Preprint. Discussion started: 25 April 2023

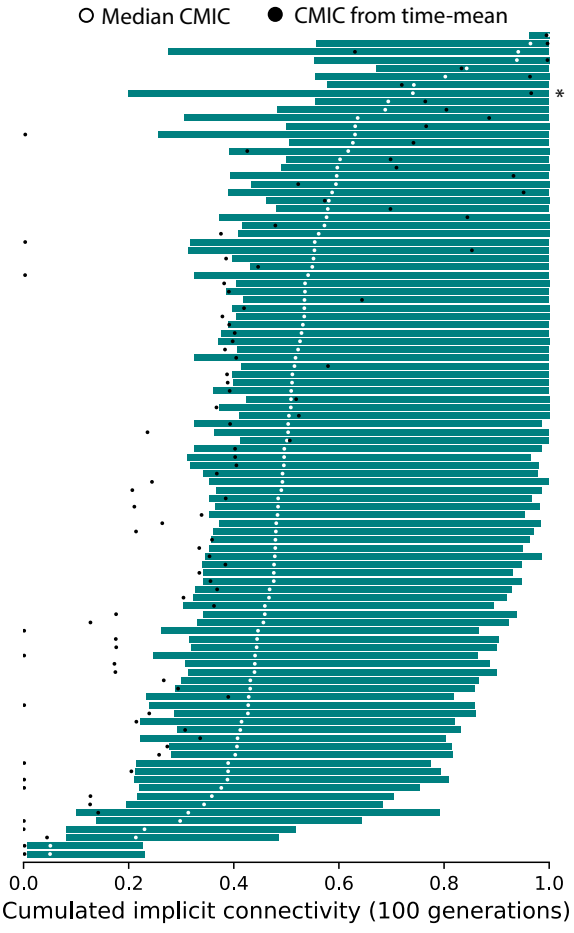

Figure 9. (Backward) cumulated multistep implicit connectivity (CMIC) over 100 steps for 100 randomly chosen connections (which have nonzero connectivity for at least 1% of spawning events). Connections for each step are selected based on a random time-slice during the northwest monsoon, and this is repeated 1000 times to obtain 1000 CMIC realisations. The teal bars show the 5^{th}-95^{th} percentiles across the 1000 realisations, and the white points represent the median. The black points represent the CMIC obtained from the time-mean potential connectivity matrix.

460 cycle). It is also questionable whether a time-mean dispersal matrix should be used to explain recent inferred gene flow (e.g. Padrón et al., 2018), when model-data mismatch (or agreement) could simply be due to stochastic variability.

4.4 Uncertainty in spawning timing does not introduce major uncertainty to connectivity predictions

There are few direct observations of spawning timing in the west Indian Ocean (Baird et al., 2021). Aside from the general observation that spawning in the southwest Indian Ocean tends to occur during the northwest monsoon (e.g. Mangubhai and

https://doi.org/10.5194/egusphere-2023-778
Preprint. Discussion started: 25 April 2023

Harrison, 2008; Mangubhai, 2009; Koester et al., 2021; Baird et al., 2021), there is no data for most coral species at most locations. This raises the important question: to what extent is this a problem for large-scale coral larval dispersal simulations?

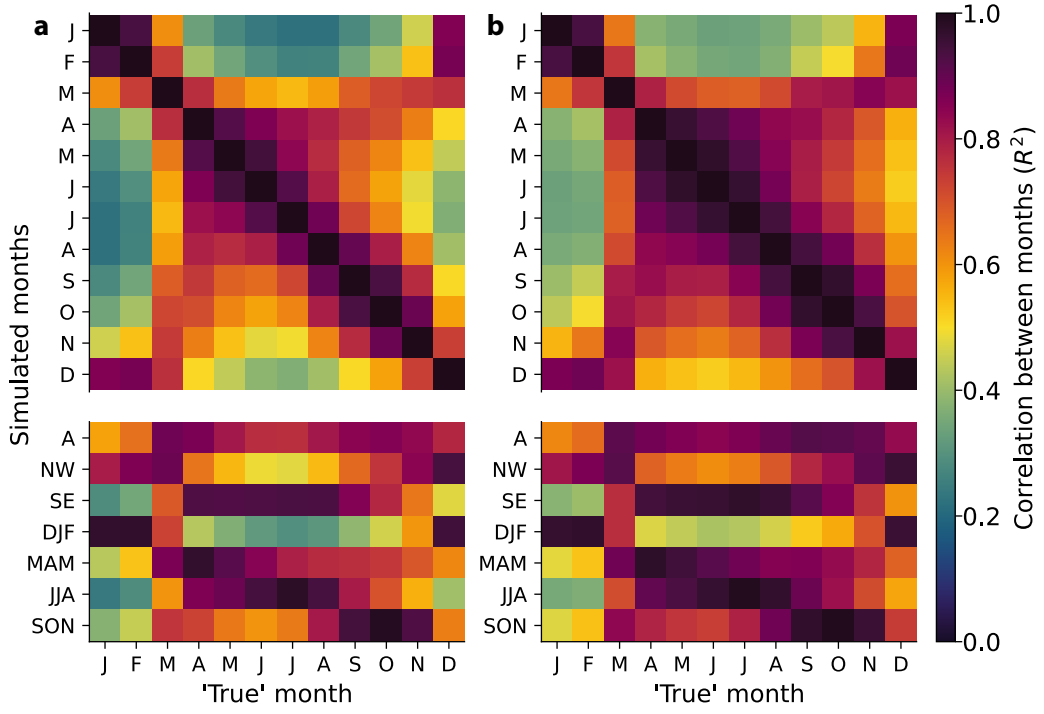

Figure 10. (a) Source strength correlation (across all reef cells) between (*top*) all pairs of months, and (*bottom*) certain combinations of months. Correlation is expressed as the R^2 value. For instance, the first row of this matrix shows the correlation (across all reef cells) for source strength averaged across January, with source strength averaged across each other month individually (columns). A high value indicates that the average source strength during January is strongly correlated with the average source strength during the column month. For the lower matrix, the combinations of months used are: (**A**) all months, i.e. annual mean source strength; (NW) northwest monsoon, here defined very broadly as October to March; (**SE**) southeast monsoon, here defined very broadly as April to September; (**DJF**) December, January, February; (**MAM**) March, April, May; (**JJA**) June, July, August; and (**SON**) September, October, November. (b) As with *(a)*, but for flux (based on groups, not cells).

As discussed throughout this paper, high-frequency variability dominates most source strength and flux time-series. As a result, the exact timing of a particular spawning event will have an enormous influence on the fate of larvae produced. This high-frequency variability is stochastic and is, for all practical purposes, impossible to predict for the vast majority of reefs. However, after a large number of spawning events, further events no longer lead to an increase in potential connectivity variability (Figure 7) and the dominant remaining signal is the seasonal cycle. If we are interested in long-term reef connectivity (decadal and beyond), it is important to understand how sensitive key connectivity metrics such as source strength and flux are to spawning timing within the seasonal cycle.

https://doi.org/10.5194/egusphere-2023-778
Preprint. Discussion started: 25 April 2023

Once high-frequency variability is filtered out (by aggregating source strength and flux by month), the correlation of (a) source strength and (b) flux between pairs of months shows a bimodal pattern, with high correlation within monsoons and lower correlation between monsoons (Figure 10). Despite the importance of the seasonal cycle, annual mean source strength and flux correlate reasonably well with corresponding metrics for all individual months, with minimum R^2 values of 0.58 and 0.62 respectively. This indicates that reefs with high (or low) time-mean source strength, or connections associated with high (or low) time-mean larval fluxes, also tend to be high (or low) for each individual month. Within individual monsoons, correlations are unsurprisingly stronger. The mean source strength (flux) for the entire northwest monsoon, here defined very loosely as October to March, correlates well with all individual constituent months, with R^2 values ranging from 0.75-0.94 (0.81-0.96). This suggests that, in the absence of any better constraints, metrics averaged over the northwest monsoon will capture the first-order patterns of potential connectivity for corals in the southwest Indian Ocean, regardless of when exactly spawning occurs during that period. Improved coverage of coral spawning data in the southwest Indian Ocean will be useful for improving potential connectivity predictions, but we do not think that this data gap prevents us from understanding large-scale connectivity patterns across the region.

5 Conclusions

Coral reef potential connectivity is highly complex, with time-mean and seasonal signals often drowned out by high-magnitude, high-frequency variability. However, we have demonstrated that there is some order within this complexity.

Within the southwest Indian Ocean, there are relatively robust oceanographic and geographic predictors of high-frequency variability in potential connectivity, which is most extreme at remote islands and atolls under the influence of rapid ocean currents, and suppressed along near-shore reefs, particularly where ocean currents tend to trap larvae against the coast. These patterns will provide marine practitioners with an initial, qualitative indication of how significant high-frequency variability in potential connectivity may be at sites of interest. Although a predictable seasonal cycle is dominant at some reefs, particularly within the EACC, our results demonstrate that, at most reefs, day-to-day variability in potential connectivity is greater in magnitude than the mean connectivity, the seasonal cycle, and interannual variability.

Since most successfully settling larvae are generated by a small minority of spawning events, studies simulating only a small number of spawning events may significantly underestimate long-term potential connectivity, particularly at remote islands. This may have particularly important consequences for predicting genetic connectivity, in which rare but 'high-impact' dispersal events may play a disproportionately important role. Reasonably characterising the potential connectivity of a relatively sparse network of reefs therefore requires a large number of spawning events, ideally over multiple decades. If this is not possible (for instance, due to the costs associated with running a high-resolution hydrodynamical model), simulating a large number of spawning events over a smaller number of years likely gives a better indication of potential connectivity variability than simulating a smaller number of spawning events over a larger number of years. Neglecting this will severely under-represent uncertainty in potential connectivity from the dispersal model. However, even with a large number of simulated spawning events, the time-mean (or seasonal) connectivity matrix alone may be of limited utility for many ecological applications, since

https://doi.org/10.5194/egusphere-2023-778
Preprint. Discussion started: 25 April 2023

the actual potential connectivity over years and even decades may deviate massively from the long-term average. Furthermore, due to uncertainty introduced by oceanographic variability, we would argue that, over sub-evolutionary timescales (and potentially even evolutionary timescales), it is fundamentally impossible to obtain anything more than first-order constraints on the importance of individual connections between reefs through marine dispersal.

Since the autocorrelation timescale for potential connectivity at most reefs is on the order of a few days, protracted spawning eliminates most variability associated with source strength, and some variability associated with the strength of individual connections. This suggests that the larval supply associated with broadcasting corals that spawn infrequently over a short duration is likely to be highly irregular, inconsistent and unpredictable, in comparison to corals carrying out split-spawning, asynchronous and protracted spawning, or continuous larval release by some brooding corals. In contrast, although constraints on spawning duration are therefore critical to reasonably characterise the variability of coral reef connectivity, the timing of spawning onset appears to be of lesser importance. In the monsoon-dominated southwest Indian Ocean, *long-term* potential connectivity patterns are relatively consistent within monsoons, with fairly low sensitivity to uncertainty in spawning timing. Even with excellent data assimilation (which is rarely available at fine scales relevant for larval dispersal), day-to-day potential connectivity variability is chaotic and stochastic, and the exact timing of spawning therefore has limited practical significance.

Code and data availability. SECoW, code, and data required to reproduce figures in this paper can be found in Supplementary Dataset 1 (Vogt-Vincent et al., 2023). Trajectory data required to recompute matrices for different parameters can be found in Supplementary Dataset 2 (*Note:* this dataset is currently being archived at the British Oceanographic Data Centre, and will be made publicly available prior to publication. We are happy to find a solution to make these available earlier to the reviewers upon request.). The hydrodynamical model output, WINDS-M (Vogt-Vincent and Johnson, 2022), can be downloaded from the CEDA archive.

Competing interests. The authors declare no competing interests.

Acknowledgements. This work was funded by NERC grant NE/S007474/1 and used the ARCHER2 UK National Supercomputing Service (https://www.archer2.ac.uk), and JASMIN, the UK collaborative data analysis facility. We are grateful to the SEA-UNICORN network, which has informed analyses carried out in this study.

.

https://doi.org/10.5194/egusphere-2023-778
Preprint. Discussion started: 25 April 2023

References

Adjeroud, M., Peignon, C., Gauliard, C., Penin, L., and Kayal, M.: Extremely high but localized pulses of coral recruitment in the southwestern lagoon of New Caledonia and implications for conservation, Marine Ecology Progress Series, 692, 67–79, https://doi.org/10.3354/meps14073, 2022.

Aguiar-González, B., Ponsoni, L., Ridderinkhof, H., van Aken, H. M., de Ruijter, W. P., and Maas, L. R.: Seasonal variation of the South Indian tropical gyre, Deep-Sea Research Part I: Oceanographic Research Papers, 110, 123–140, https://doi.org/10.1016/j.dsr.2016.02.004, publisher: Elsevier, 2016.

Auclair, F., Benshila, R., Bordois, L., Boutet, M., Brémond, M., Caillaud, M., Cambon, G., Capet, X., Debreu, L., Ducousso, N., Dufois, F., Dumas, F., Ethé, C., Gula, J., Hourdin, C., Illig, S., Jullien, S., Corre, M. L., Gac, S. L., Gentil, S. L., Lemarié, F., Marchesiello, P., Mazoyer, C., Morvan, G., Nguyen, C., Penven, P., Person, R., Pianezze, J., Pous, S., Renault, L., Roblou, L., Sepulveda, A., and Theetten, S.: Coastal and Regional Ocean COmmunity model, https://doi.org/10.5281/zenodo.7415133, 2019.

Baird, A. H., Guest, J. R., and Willis, B. L.: Systematic and Biogeographical Patterns in the Reproductive Biology of Scleractinian Corals, Annual Review of Ecology, Evolution, and Systematics, 40, 551–571, https://doi.org/10.1146/annurev.ecolsys.110308.120220, 2009.

Baird, A. H., Guest, J. R., Edwards, A. J., Bauman, A. G., Bouwmeester, J., Mera, H., Abrego, D., Alvarez-Noriega, M., Babcock, R. C., Barbosa, M. B., Bonito, V., Burt, J., Cabaitan, P. C., Chang, C.-F., Chavanich, S., Chen, C. A., Chen, C.-J., Chen, W.-J., Chung, F.-C., Connolly, S. R., Cumbo, V. R., Dornelas, M., Doropoulos, C., Eyal, G., Eyal-Shaham, L., Fadli, N., Figueiredo, J., Flot, J.-F., Gan, S.-H., Gomez, E., Graham, E. M., Grinblat, M., Gutiérrez-Isaza, N., Harii, S., Harrison, P. L., Hatta, M., Ho, N. A. J., Hoarau, G., Hoogenboom, M., Howells, E. J., Iguchi, A., Isomura, N., Jamodiong, E. A., Jandang, S., Keyse, J., Kitanobo, S., Kongjandtre, N., Kuo, C.-Y., Ligson, C., Lin, C.-H., Low, J., Loya, Y., Maboloc, E. A., Madin, J. S., Mezaki, T., Min, C., Morita, M., Moya, A., Neo, S.-H., Nitschke, M. R., Nojima, S., Nozawa, Y., Piromvaragorn, S., Plathong, S., Puill-Stephan, E., Quigley, K., Ramirez-Portilla, C., Ricardo, G., Sakai, K., Sampayo, E., Shlesinger, T., Sikim, L., Simpson, C., Sims, C. A., Sinniger, F., Spiji, D. A., Tabalanza, T., Tan, C.-H., Terraneo, T. I., Torda, G., True, J., Tun, K., Vicentuan, K., Viyakarn, V., Waheed, Z., Ward, S., Willis, B., Woods, R. M., Woolsey, E. S., Yamamoto, H. H., and Yusuf, S.: An Indo-Pacific coral spawning database, Scientific Data, 8, 35, https://doi.org/10.1038/s41597-020-00793-8, 2021.

Balbar, A. C. and Metaxas, A.: The current application of ecological connectivity in the design of marine protected areas, Global Ecology and Conservation, 17, e00 569, https://doi.org/10.1016/j.gecco.2019.e00569, publisher: Elsevier Ltd, 2019.

Bastidas, C., Cróquer, A., Zubillaga, A. L., Ramos, R., Kortnik, V., Weinberger, C., and Márquez, L. M.: Coral mass- and split-spawning at a coastal and an offshore Venezuelan reefs, southern Caribbean, Hydrobiologia, 541, 101–106, https://doi.org/10.1007/s10750-004-4672-y, 2005.

Bronstein, O. and Loya, Y.: Daytime spawning of Porites rus on the coral reefs of Chumbe Island in Zanzibar, Western Indian Ocean (WIO), Coral Reefs, 30, 441–441, https://doi.org/10.1007/s00338-011-0733-7, 2011.

Connolly, S. R. and Baird, A. H.: Estimating dispersal potential for marine larvae: Dynamic models applied to scleractinian corals, Ecology, 91, 3572–3583, https://doi.org/10.1890/10-0143.1, 2010.

Dauhajre, D. P., McWilliams, J. C., and Renault, L.: Nearshore Lagrangian Connectivity: Submesoscale Influence and Resolution Sensitivity, Journal of Geophysical Research: Oceans, 124, 5180–5204, https://doi.org/10.1029/2019JC014943, 2019.

Delandmeter, P. and van Sebille, E.: The Parcels v2.0 Lagrangian framework: new field interpolation schemes, Geoscientific Model Development Discussions, pp. 1–24, https://doi.org/10.5194/gmd-2018-339, 2019.

https://doi.org/10.5194/egusphere-2023-778
Preprint. Discussion started: 25 April 2023

Doropoulos, C. and Roff, G.: Coloring coral larvae allows tracking of local dispersal and settlement, PLOS Biology, 20, e3001 907, https://doi.org/10.1371/journal.pbio.3001907, 2022.

Edmunds, P. J., McIlroy, S. E., Adjeroud, M., Ang, P., Bergman, J. L., Carpenter, R. C., Coffroth, M. A., Fujimura, A. G., Hench, J. L., Holbrook, S. J., Leichter, J. J., Muko, S., Nakajima, Y., Nakamura, M., Paris, C. B., Schmitt, R. J., Sutthacheep, M., Toonen, R. J., Sakai, K., Suzuki, G., Washburn, L., Wyatt, A. S. J., and Mitarai, S.: Critical Information Gaps Impeding Understanding of the Role of Larval Connectivity Among Coral Reef Islands in an Era of Global Change, Frontiers in Marine Science, 5, 1–16, https://doi.org/10.3389/fmars.2018.00290, 2018.

Egbert, G. D. and Erofeeva, S. Y.: Efficient inverse modeling of barotropic ocean tides, Journal of Atmospheric and Oceanic Technology, 19, 183–204, https://doi.org/10.1175/1520-0426(2002)019<0183:EIMOBO>2.0.CO;2, 2002.

Faubet, P., Waples, R. S., and Gaggiotti, O. E.: Evaluating the performance of a multilocus Bayesian method for the estimation of migration rates: EVALUATING THE PERFORMANCE OF BAYESIAN METHODS, Molecular Ecology, 16, 1149–1166, https://doi.org/10.1111/j.1365-294X.2007.03218.x, 2007.

Figueiredo, J., Thomas, C. J., Deleersnijder, E., Lambrechts, J., Baird, A. H., Connolly, S. R., and Hanert, E.: Global warming decreases connectivity among coral populations, Nature Climate Change, 12, 83–87, https://doi.org/10.1038/s41558-021-01248-7, publisher: Springer US, 2022.

Foster, N. L., Paris, C. B., Kool, J. T., Baums, I. B., Stevens, J. R., Sanchez, J. A., Bastidas, C., Agudelo, C., Bush, P., Day, O., Ferrari, R., Gonzalez, P., Gore, S., Guppy, R., McCartney, M. A., McCoy, C., Mendes, J., Srinivasan, A., Steiner, S., Vermeij, M. J., Weil, E., and Mumby, P. J.: Connectivity of Caribbean coral populations: Complementary insights from empirical and modelled gene flow, Molecular Ecology, 21, 1143–1157, https://doi.org/10.1111/j.1365-294X.2012.05455.x, 2012.

Foster, T., Heyward, A. J., and Gilmour, J. P.: Split spawning realigns coral reproduction with optimal environmental windows, Nature Communications, 9, 718, https://doi.org/10.1038/s41467-018-03175-2, 2018.

Galindo, H. M., Olson, D. B., and Palumbi, S. R.: Seascape Genetics: A Coupled Oceanographic-Genetic Model Predicts Population Structure of Caribbean Corals, Current Biology, 16, 1622–1626, https://doi.org/10.1016/j.cub.2006.06.052, 2006.

Gamoyo, M., Obura, D., and Reason, C. J.: Estimating Connectivity Through Larval Dispersal in the Western Indian Ocean, Journal of Geophysical Research: Biogeosciences, 124, 2446–2459, https://doi.org/10.1029/2019JG005128, 2019.

Geertsma, R., Kamermans, P., Murk, A., and Wijgerde, T.: Real-time high resolution tracking of coral and oyster larvae, Journal of Experimental Marine Biology and Ecology, 565, 151 910, https://doi.org/10.1016/j.jembe.2023.151910, 2023.

Goetze, J. S., Wilson, S., Radford, B., Fisher, R., Langlois, T. J., Monk, J., Knott, N. A., Malcolm, H., Currey-Randall, L. M., Ierodiaconou, D., Harasti, D., Barrett, N., Babcock, R. C., Bosch, N. E., Brock, D., Claudet, J., Clough, J., Fairclough, D. V., Heupel, M. R., Holmes, T. H., Huveneers, C., Jordan, A. R., McLean, D., Meekan, M., Miller, D., Newman, S. J., Rees, M. J., Roberts, K. E., Saunders, B. J., Speed, C. W., Travers, M. J., Treml, E., Whitmarsh, S. K., Wakefield, C. B., and Harvey, E. S.: Increased connectivity and depth improve the effectiveness of marine reserves, Global Change Biology, 27, 3432–3447, https://doi.org/10.1111/gcb.15635, 2021.

Gouezo, M., Golbuu, Y., Fabricius, K., Olsudong, D., Mereb, G., Nestor, V., Wolanski, E., Harrison, P., and Doropoulos, C.: Drivers of recovery and reassembly of coral reef communities, Proceedings of the Royal Society B: Biological Sciences, 286, https://doi.org/10.1098/rspb.2018.2908, iSBN: 0000000180382, 2019.

Graham, E. M., Baird, A. H., and Connolly, S. R.: Survival dynamics of scleractinian coral larvae and implications for dispersal, Coral Reefs, 27, 529–539, https://doi.org/10.1007/s00338-008-0361-z, 2008.

https://doi.org/10.5194/egusphere-2023-778
Preprint. Discussion started: 25 April 2023

Green, R. H., Lowe, R. J., and Buckley, M. L.: Hydrodynamics of a Tidally Forced Coral Reef Atoll, Journal of Geophysical Research: Oceans, 123, 7084–7101, https://doi.org/10.1029/2018JC013946, 2018.

Grimaldi, C. M., Lowe, R. J., Benthuysen, J. A., Cuttler, M. V. W., Green, R. H., Radford, B., Ryan, N., and Gilmour, J.: Hydrodynamic drivers of fine-scale connectivity within a coral reef atoll, Limnology and Oceanography, pp. 1–14, https://doi.org/10.1002/lno.12198, 2022.

Harrison, C. S., Siegel, D. A., and Mitarai, S.: Filamentation and eddy-eddy interactions in marine larval accumulation and transport, Marine Ecology Progress Series, 472, 27–44, https://doi.org/10.3354/meps10061, 2013.

Harrison, H. B., Bode, M., Williamson, D. H., Berumen, M. L., and Jones, G. P.: A connectivity portfolio effect stabilizes marine reserve performance, Proceedings of the National Academy of Sciences of the United States of America, 117, 25 595–25 600, https://doi.org/10.1073/pnas.1920580117, 2020.

Harrison, P. L.: Sexual Reproduction of Scleractinian Corals, in: Coral Reefs: an Ecosystem in Transition, pp. 59–85, Springer Netherlands, 1 edn., 2010.

Hartmann, A. C., Marhaver, K. L., and Vermeij, M. J.: Corals in Healthy Populations Produce More Larvae Per Unit Cover, Conservation Letters, 11, 1–12, https://doi.org/10.1111/conl.12410, 2018.

Hata, T., Madin, J. S., Cumbo, V. R., Denny, M., Figueiredo, J., Harii, S., Thomas, C. J., and Baird, A. H.: Coral larvae are poor swimmers and require fine-scale reef structure to settle, Scientific Reports, 7, 1–9, https://doi.org/10.1038/s41598-017-02402-y, publisher: Springer US, 2017.

Hersbach, H., Bell, B., Berrisford, P., Hirahara, S., Horányi, A., Muñoz-Sabater, J., Nicolas, J., Peubey, C., Radu, R., Schepers, D., Simmons, A., Soci, C., Abdalla, S., Abellan, X., Balsamo, G., Bechtold, P., Biavati, G., Bidlot, J., Bonavita, M., De Chiara, G., Dahlgren, P., Dee, D., Diamantakis, M., Dragani, R., Flemming, J., Forbes, R., Fuentes, M., Geer, A., Haimberger, L., Healy, S., Hogan, R. J., Hólm, E., Janisková, M., Keeley, S., Laloyaux, P., Lopez, P., Lupu, C., Radnoti, G., de Rosnay, P., Rozum, I., Vamborg, F., Villaume, S., and Thépaut, J. N.: The ERA5 global reanalysis, Quarterly Journal of the Royal Meteorological Society, 146, 1999–2049, https://doi.org/10.1002/qj.3803, 2020.

Hock, K., Wolff, N. H., Ortiz, J. C., Condie, S. A., Anthony, K. R., Blackwell, P. G., and Mumby, P. J.: Connectivity and systemic resilience of the Great Barrier Reef, PLoS Biology, 15, 1–23, https://doi.org/10.1371/journal.pbio.2003355, iSBN: 1111111111, 2017.

Hock, K., Doropoulos, C., Gorton, R., Condie, S. A., and Mumby, P. J.: Split spawning increases robustness of coral larval supply and inter-reef connectivity, Nature Communications, 10, 1–10, https://doi.org/10.1038/s41467-019-11367-7, publisher: Springer US, 2019.

Holstein, D. M., Smith, T. B., van Hooidonk, R., and Paris, C. B.: Predicting coral metapopulation decline in a changing thermal environment, Coral Reefs, 41, 961–972, https://doi.org/10.1007/s00338-022-02252-9, 2022.

Horoiwa, M., Nakamura, T., Yuasa, H., Kajitani, R., Ameda, Y., Sasaki, T., Taninaka, H., Kikuchi, T., Yamakita, T., Toyoda, A., Itoh, T., and Yasuda, N.: Integrated Population Genomic Analysis and Numerical Simulation to Estimate Larval Dispersal of Acanthaster cf. solaris Between Ogasawara and Other Japanese Regions, Frontiers in Marine Science, 8, 1–12, https://doi.org/10.3389/fmars.2021.688139, 2022.

Kingsford, M. J., Leis, J. M., Shanks, A., Lindeman, K. C., Morgan, S. G., and Pineda, J.: Sensory environments, larval abilities, and local self-recruitment, BULLETIN OF MARINE SCIENCE, 70, 2002.

Kleypas, J. A., Thompson, D. M., Castruccio, F. S., Curchitser, E. N., Pinsky, M., and Watson, J. R.: Larval connectivity across temperature gradients and its potential effect on heat tolerance in coral populations, Global Change Biology, 22, 3539–3549, https://doi.org/10.1111/gcb.13347, 2016.

https://doi.org/10.5194/egusphere-2023-778
Preprint. Discussion started: 25 April 2023

Koester, A., Ford, A. K., Ferse, S. C., Migani, V., Bunbury, N., Sanchez, C., and Wild, C.: First insights into coral recruit and juvenile abundances at remote Aldabra Atoll, Seychelles, PLoS ONE, 16, 1–19, https://doi.org/10.1371/journal.pone.0260516, iSBN: 1111111111, 2021.

Kough, A. S. and Paris, C. B.: The influence of spawning periodicity on population connectivity, Coral Reefs, 34, 753–757, https://doi.org/10.1007/s00338-015-1311-1, publisher: Springer Berlin Heidelberg, 2015.

Lange, M. and van Sebille, E.: Parcels v0.9: Prototyping a Lagrangian ocean analysis framework for the petascale age, Geoscientific Model Development, 10, 4175–4186, https://doi.org/10.5194/gmd-10-4175-2017, arXiv: 1707.05163, 2017.

Largier, J. L.: Considerations in estimating larval dispersal distances from oceanographic data, Ecological Applications, 13, 71–89, https://doi.org/10.1890/1051-0761(2003)013[0071:cieldd]2.0.co;2, 2003.

Legrand, T., Chenuil, A., Ser-giacomi, E., Arnaud-haond, S., Bierne, N., Rossi, V., Legrand, T., Chenuil, A., Ser-giacomi, E., Arnaud-haond, S., and Bierne, N.: Spatial coalescent connectivity through multi-generation dispersal modelling predicts gene flow across marine phyla, Nature Communications, 13, 5861, https://doi.org/10.1038/s41467-022-33499-z, publisher: Springer US, 2022.

Leinbach, S. E., Speare, K. E., Rossin, A. M., Holstein, D. M., and Strader, M. E.: Energetic and reproductive costs of coral recovery in divergent bleaching responses, Scientific Reports, 11, 23 546, https://doi.org/10.1038/s41598-021-02807-w, 2021.

Lellouche, J.-M., Greiner, E., Bourdallé Badie, R., Garric, G., Melet, A., Drévillon, M., Bricaud, C., Hamon, M., Le Galloudec, O., Regnier, C., Candela, T., Testut, C.-E., Gasparin, F., Ruggiero, G., Benkiran, M., Drillet, Y., and Le Traon, P.-Y.: The Copernicus Global 1/12° Oceanic and Sea Ice GLORYS12 Reanalysis, Frontiers in Earth Science, 9, 1–27, https://doi.org/10.3389/feart.2021.698876, 2021.

Levitan, D., Boudreau, W., Jara, J., and Knowlton, N.: Long-term reduced spawning in Orbicella coral species due to temperature stress, Marine Ecology Progress Series, 515, 1–10, https://doi.org/10.3354/meps11063, 2014.

Lowe, W. H. and Allendorf, F. W.: What can genetics tell us about population connectivity?, Molecular Ecology, 19, 3038–3051, https://doi.org/10.1111/j.1365-294X.2010.04688.x, 2010.

Mangubhai, S.: Reproductive ecology of the scleractinian corals *Echinopora gemmacea* and *Leptoria phrygia* (Faviidae) on equatorial reefs in Kenya, Invertebrate Reproduction & Development, 53, 67–79, https://doi.org/10.1080/07924259.2009.9652292, 2009.

Mangubhai, S. and Harrison, P.: Asynchronous coral spawning patterns on equatorial reefs in Kenya, Marine Ecology Progress Series, 360, 85–96, https://doi.org/10.3354/meps07385, 2008.

Mangubhai, S. and Harrison, P.: Extended breeding seasons and asynchronous spawning among equatorial reef corals in Kenya, Marine Ecology Progress Series, 374, 305–310, https://doi.org/10.3354/meps07910, 2009.

Mangubhai, S., Harris, A., and Graham, N. A. J.: Synchronous daytime spawning of the solitary coral Fungia danai (Fungiidae) in the Chagos Archipelago, central Indian Ocean, Coral Reefs, 26, 15–15, https://doi.org/10.1007/s00338-006-0173-y, 2007.

Manyilizu, M., Penven, P., and Reason, C. J.: Annual cycle of the upper-ocean circulation and properties in the tropical western Indian Ocean, African Journal of Marine Science, 38, 81–99, https://doi.org/10.2989/1814232X.2016.1158123, 2016.

Mayorga-Adame, C. G., Ted Strub, P., Batchelder, H. P., and Spitz, Y. H.: Characterizing the circulation off the Kenyan-Tanzanian coast using an ocean model, Journal of Geophysical Research: Oceans, 121, 1377–1399, https://doi.org/10.1002/2015JC010860, iSBN: 2169-9291, 2016.

Mayorga-Adame, C. G., Batchelder, H. P., and Spitz, Y. H.: Modeling larval connectivity of coral reef organisms in the Kenya-Tanzania region, Frontiers in Marine Science, 4, https://doi.org/10.3389/fmars.2017.00092, 2017.

https://doi.org/10.5194/egusphere-2023-778
Preprint. Discussion started: 25 April 2023

McManus, L. C., Forrest, D. L., Tekwa, E. W., Schindler, D. E., Colton, M. A., Webster, M. M., Essington, T. E., Palumbi, S. R., Mumby, P. J., and Pinsky, M. L.: Evolution and connectivity influence the persistence and recovery of coral reefs under climate change in the Caribbean, Southwest Pacific, and Coral Triangle, Global Change Biology, pp. 1–15, https://doi.org/10.1111/gcb.15725, 2021.

Mitarai, S., Siegel, D. A., and Winters, K. B.: A numerical study of stochastic larval settlement in the California Current system, Journal of Marine Systems, 69, 295–309, https://doi.org/10.1016/j.jmarsys.2006.02.017, 2008.

Nagura, M. and McPhaden, M. J.: Dynamics of zonal current variations associated with the Indian Ocean dipole, Journal of Geophysical Research: Oceans, 115, 1–12, https://doi.org/10.1029/2010JC006423, 2010.

Nakamura, M., Murakami, T., Kohno, H., Mizutani, A., and Shimokawa, S.: Rapid recovery of coral communities from a mass bleaching event in the summer of 2016, observed in Amitori Bay, Iriomote Island, Japan, Marine Biology, 169, 104, https://doi.org/10.1007/s00227-022-04091-2, 2022.

Nozawa, Y. and Harrison, P. L.: Effects of elevated temperature on larval settlement and post-settlement survival in scleractinian corals, Acropora solitaryensis and Favites chinensis, Marine Biology, 152, 1181–1185, https://doi.org/10.1007/s00227-007-0765-2, 2007.

Padrón, M., Costantini, F., Baksay, S., Bramanti, L., and Guizien, K.: Passive larval transport explains recent gene flow in a Mediterranean gorgonian, Coral Reefs, 37, 495–506, https://doi.org/10.1007/s00338-018-1674-1, 2018.

Painter, S. C.: The biogeochemistry and oceanography of the East African Coastal Current, Progress in Oceanography, 186, 102 374, https://doi.org/10.1016/j.pocean.2020.102374, publisher: Elsevier, 2020.

Painter, S. C., Sekadende, B., Michael, A., Noyon, M., Shayo, S., Godfrey, B., Mwadini, M., and Kyewalyanga, M.: Evidence of localised upwelling in Pemba Channel (Tanzania) during the southeast monsoon, Ocean & Coastal Management, 200, 105 462, https://doi.org/10.1016/j.ocecoaman.2020.105462, 2021.

Porter, S. N. and Schleyer, M. H.: Long-term dynamics of a high-latitude coral reef community at Sodwana Bay, South Africa, Coral Reefs, 36, 369–382, https://doi.org/10.1007/s00338-016-1531-z, 2017.

Pratchett, M. S., Hoey, A. S., Tan, C.-H., Kuo, C.-Y., Bauman, A. G., Kumaraswamy, R., and Baird, A. H.: Spatial and Temporal Variation in Fecundity of Acropora spp. in the Northern Great Barrier Reef, Diversity, 11, 60, https://doi.org/10.3390/d11040060, 2019.

Romero, L., Uchiyama, Y., Ohlmann, J. C., McWilliams, J. C., and Siegel, D. A.: Simulations of Nearshore Particle-Pair Dispersion in Southern California, Journal of Physical Oceanography, 43, 1862–1879, https://doi.org/10.1175/JPO-D-13-011.1, 2013.

Sachidanandan, C., Lengaigne, M., Muraleedharan, P. M., and Mathew, B.: Interannual variability of zonal currents in the equatorial Indian Ocean: respective control of IOD and ENSO, Ocean Dynamics, 67, 857–873, https://doi.org/10.1007/s10236-017-1061-4, publisher: Ocean Dynamics ISBN: 1023601710, 2017.

Samarasin, P., Shuter, B. J., Wright, S. I., and Rodd, F. H.: The problem of estimating recent genetic connectivity in a changing world: Recent Genetic Connectivity, Conservation Biology, 31, 126–135, https://doi.org/10.1111/cobi.12765, 2017.

Schott, F. A. and McCreary, J. P.: The monsoon circulation of the Indian Ocean, Progress in Oceanography, 51, 1–123, https://doi.org/10.1016/S0079-6611(01)00083-0, 2001.

Schott, F. A., Xie, S. P., and McCreary, J. P.: Indian ocean circulation and climate variability, Reviews of Geophysics, 47, 1–46, https://doi.org/10.1029/2007RG000245, 2009.

Ser-Giacomi, E., Legrand, T., Hernández-Carrasco, I., and Rossi, V.: Explicit and implicit network connectivity: Analytical formulation and application to transport processes, Physical Review E, 103, 1–15, https://doi.org/10.1103/PhysRevE.103.042309, arXiv: 2104.02537 Publisher: American Physical Society, 2021.

https://doi.org/10.5194/egusphere-2023-778
Preprint. Discussion started: 25 April 2023

Siegel, D. A., Mitarai, S., Costello, C. J., Gaines, S. D., Kendall, B. E., Warner, R. R., and Winters, K. B.: The stochastic nature of larval connectivity among nearshore marine populations, Proceedings of the National Academy of Sciences, 105, 8974–8979, https://doi.org/10.1073/pnas.0802544105, 2008.

Sola, E., Marques da Silva, I., and Glassom, D.: Spatio-temporal patterns of coral recruitment at Vamizi Island, Quirimbas Archipelago, Mozambique, African Journal of Marine Science, 37, 557–565, https://doi.org/10.2989/1814232X.2015.1113201, 2015.

Sola, E., Marques da Silva, I., and Glassom, D.: Reproductive synchrony in a diverse *Acropora* assemblage, Vamizi Island, Mozambique, Marine Ecology, 37, 1373–1385, https://doi.org/10.1111/maec.12348, 2016.

Swallow, J. C., Schott, F., and Fieux, M.: Structure and transport of the East African Coastal Current, Journal of Geophysical Research, 96, 22 245, https://doi.org/10.1029/91jc01942, 1991.

Thompson, D. M., Kleypas, J., Castruccio, F., Curchitser, E. N., Pinsky, M. L., Jönsson, B., and Watson, J. R.: Variability in oceanographic barriers to coral larval dispersal: Do currents shape biodiversity?, Progress in Oceanography, 165, 110–122, https://doi.org/10.1016/j.pocean.2018.05.007, publisher: Elsevier, 2018.

Thomson, D. P., Babcock, R. C., Evans, R. D., Feng, M., Moustaka, M., Orr, M., Slawinski, D., Wilson, S. K., and Hoey, A. S.: Coral larval recruitment in north-western Australia predicted by regional and local conditions, Marine Environmental Research, 168, 105 318, https://doi.org/10.1016/j.marenvres.2021.105318, 2021.

Treml, E. A., Halpin, P. N., Urban, D. L., and Pratson, L. F.: Modeling population connectivity by ocean currents, a graph-theoretic approach for marine conservation, Landscape Ecology, 23, 19–36, https://doi.org/10.1007/s10980-007-9138-y, 2008.

Vogt-Vincent, N. and Johnson, H.: WINDS-M: A 1/50° multidecadal regional simulation of the Southwestern Indian Ocean with high frequency surface currents for Lagrangian applications (realistic forcing, 1993-2020), CEDA Archive, https://doi.org/10.5285/BF6F0CFBD09E47498572F21081376702, type: dataset, 2022.

Vogt-Vincent, N. S. and Johnson, H. L.: Multidecadal and climatological surface current simulations for the southwestern Indian Ocean at 1/50° resolution, Geoscientific Model Development, 16, 1163–1178, https://doi.org/10.5194/gmd-16-1163-2023, 2023.

Vogt-Vincent, N. S., Johnson, H. L., and Mitarai, S.: Supplementary Dataset 1 for: High-frequency variability dominates potential connectivity between remote coral reefs, https://doi.org/10.5281/zenodo.7825516, tex.entrytype: dataset tex.version: 0.1, 2023.

Watson, J. R., Kendall, B. E., Siegel, D. A., and Mitarai, S.: Changing seascapes, stochastic connectivity, and marine metapopulation dynamics, American Naturalist, 180, 99–112, https://doi.org/10.1086/665992, 2012.

Willis, B., Babcock, R., Harrison, P., Oliver, J., and Wallace, C.: Patterns in the mass spawning of corals on the Great Barrier Reef from 1981 to 1984, in: Proceedings of the 5th International Coral Reef Congress, vol. 4, pp. 343–348, Tahiti, 1985.

Wood, S., Paris, C. B., Ridgwell, A., and Hendy, E. J.: Modelling dispersal and connectivity of broadcast spawning corals at the global scale, Global Ecology and Biogeography, 23, 1–11, https://doi.org/10.1111/geb.12101, 2014.

Wood, S., Baums, I. B., Paris, C. B., Ridgwell, A., Kessler, W. S., and Hendy, E. J.: El Niño and coral larval dispersal across the eastern Pacific marine barrier, Nature Communications, 7, 12 571, https://doi.org/10.1038/ncomms12571, 2016.

Yamagami, Y. and Tozuka, T.: Interannual variability of South Equatorial Current bifurcation and western boundary currents along the Madagascar coast, Journal of Geophysical Research: Oceans, 120, 8551–8570, https://doi.org/10.1002/2015JC011069, 2015.